1. Overview of the Topic

Foams can be defined as uniform dispersions of a gaseous phase in either a liquid or a solid (Figure 1.1). The term ‘‘foam’’ is generally used for dispersion of gas bubbles in a liquid. If the morphology of such foams, however, can be preserved by letting the liquid solidify as it is, obtains a material which is called a ‘‘solid foam’’. Solid foams are a special case of what is more commonly called as ‘‘cellular solids’’.

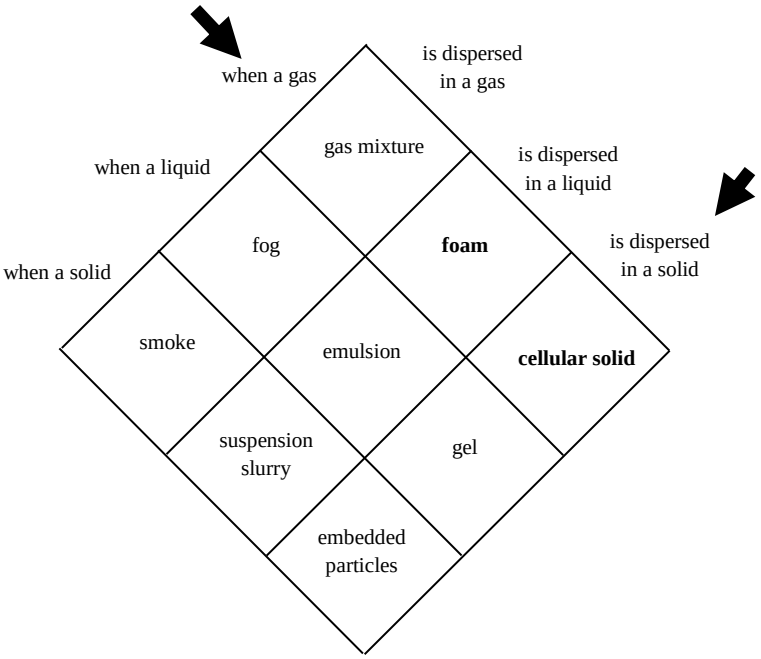

Figure 1.1: Dispersions of one phase into a second phase

The use of cellular materials allows the simultaneous optimization of stiffness, strength, overall weight, thermal conductivity, surface area, and gas permeability. As such, these materials are highly desirable for a wide range of engineering applications. Cellular materials are the most efficient structure for many applications, and are the most common engineering material form in the natural world (e.g. wood and bone). Until recently, however, only wood was used to any great extent. Only during the twentieth century have man-made polymer foams been available for insulation, cushioning, padding, and packaging, but the high structural efficiency of cellular materials has been little used. A lack of engineering design familiarity with cellular materials, and a limited ability to tailor foams fabricated from engineering materials, have contributed to the lack of development of cellular structures.

Techniques now exist for fabricating foams not only of polymers, but of **metals**, ceramics, and glasses as well. These newer foams are increasingly being used structurally, for insulation, and in systems for absorbing the kinetic energy of impacts. Their uses exploit the unique combination of properties offered by cellular solids, properties that ultimately derive from the cellular structure of the material.

Several techniques are used to produce engineering (structural) foams. With the exception of syntactic foams and self-foamed materials such as foam glass, these materials are produced using a foamed polymer as the starting material. From these economical precursors, three processing routes have been established for the production of ceramic and metallic foams.

A **'Metal Foam'** is similar to any other foam (like foam made by washing-up liquid, the inside of Aero chocolates, the yellow plastic foam in furniture), but made of a metal. Typically between 75 and 95% of the structure is made of pores, which can be connected together (giving an open-cell foam, made mainly of struts), or sealed (giving a closed-cell foam, made of separate cells which trap gas inside the metal).

Metal foams are rigid (unlike plastic foams) and can look a lot like solid metal until it is being cut (or picked it up and realize how light they are). The reason that metal foams are useful is that they have a high strength and stiffness for a given weight (note that they are generally made of aluminium due to its low density). They're also good at absorbing large amounts of energy at low stress when crushed.

The ways of making foamed metals can be divided into four broad categories.

a) The first is that of foams which are really just combinations of materials which happen to give a lot of open space - for example, metal **powders** or fibres which have been **compressed together**. The foams made by these methods tend to be of fairly poor quality.
b) A far more reliable type of process is **infiltration**, where some sort of solid mould of pore shapes is made and molten metal is poured in between them, with subsequent removal of the mould. This method tends to give highly uniform open-cell foam structures. The downside of these processes is that they are generally expensive and complicated, and only suitable for making fairly small quantities of foam.

c) Another set of processes is based on **powder processing** - powdered metal and foaming agents (i.e. some sort of chemical which will react to give off a gas) are mixed together and compressed; subsequent heating the mixture above the metal melting temperature produces a foam.

d) The cheapest process is **melt-route processing**, where some sort of gas is injected into a viscous molten metal, and is trapped in to form pores, with the metal then cooling and solidifying to form a foam. Although cheap and relatively simple; consistently obtaining a cell structure with a reasonably high quality is difficult, which has given rise to various adaptations to control the cells more closely.

There are other methods, though they tend to produce foams with a lower porosity or of lower quality. For example the **GASAR process** (invented at the Ukraine State Metallurgical Academy in 1993) involves rapid cooling of metal saturated with hydrogen. When the metal solidifies, the hydrogen is rejected and forms pores. Because the cooling happens in a particular direction, the pores are very long and parallel in the direction of cooling (and it's arguable that these materials are honeycombs rather than foams).

To date, a survey comprising over 70 questionnaires about the required research work of metal foams have been completed by **The University of California, San Diego, La Jolla, CA 92037** and the results are presented in the figure 1.2.

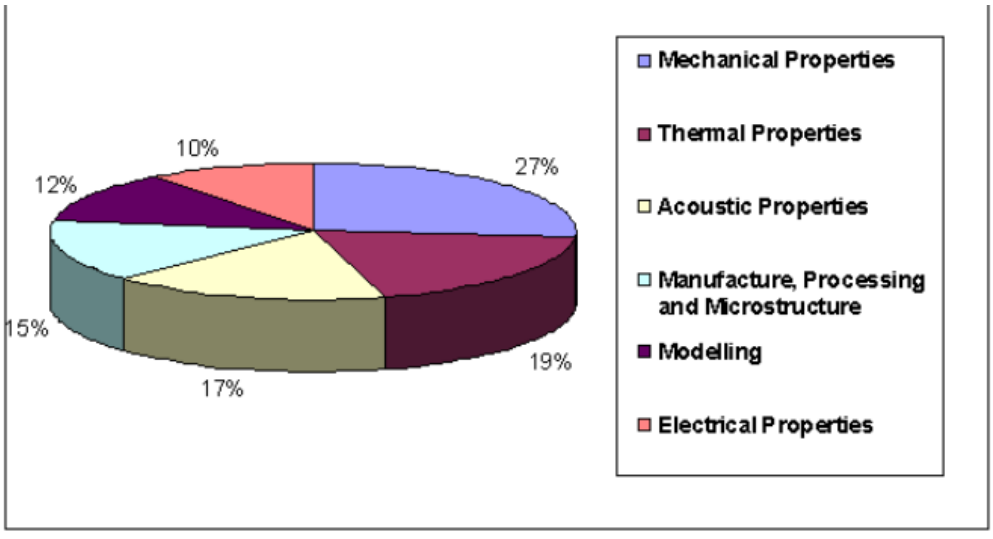

Figure 1.2: Need of foam-property characterization.

Therefore, the research work will concentrate on Mechanical, Electrical and processing properties. (more than 60%)

According to Prof. M. F. Ashby, University of Cambridge "*When modern man builds large load-bearing structures, he uses dense solids; steel, concrete, glass. When nature does the same, she generally uses cellular materials; wood, bone, coral. There must be good reasons for it.*"

Metallic foams are a relatively new class of material that offers manufacturers significant potential for lightweight structures, for energy absorption and for thermal management.

Interest in the applications of these materials is increasing rapidly throughout U. K. and U.S.A. and currently organisations embarking on many large research programmes in this area. The objective of the project is to assessing and prioritising the measurement needs associated with this new and important class of material.

Metal foam is known to exhibit multifunctional behaviour. They offer a unique combination of several properties that cannot be achieved by one conventional material at the same time such as ultra-low density, high stiffness and capability to absorb crash energy, and excellent sound absorption properties. These unique combinations of properties indicate various potential applications. The high porosity of metallic foams can absorb a large quantity of mechanical energy when they are deformed. This material can undergo large amount of deformation while stresses are limited to the compression strength of the material. Foams can therefore act as impact energy absorbers which limit accelerations in crash situations. The excellent sound absorption property of metallic foams coupled with their better mechanical properties makes this material ideally suitable for sound absorption under difficult situations, for reducing sound pollution.

2. Introduction

Intensified research in the field of metal foam resulted in a huge volume of metal foam literatures. Extensive literature survey has been carried out to find the current state of research in the field. All the available literatures have been classified into three categories; metal foam production, properties and applications. As such the entire literature survey is divided in to three sections: Characteristics of existing metal foams, Production methods of metal foams, and Application of metal foams

2.1 What is Metal Foam?

Metal foam is a cellular structure consisting of a solid metal, frequently aluminium, containing a large volume fraction of gas-filled pores. The pores can be sealed (closed-cell foam), or they can form an interconnected network (open-cell foam). The defining characteristic of metal foams is a very high porosity: typically 75–95% of the volume consists of void spaces. The strength of foamed metal possesses a power law relationship to its density; i.e., a 20% dense material is more than twice as strong as 10% dense material .Metallic foams typically retain some physical properties of their base material. The foam is generally recyclable back to its base material .Coefficient of thermal expansion will also remain similar while thermal conductivity will likely be reduced.

Figure.2.1. Metal Foam

2.2 Types of Metal Foam: Structurally, there are two basic types of metal foam.

2.2.1 Open-cell metal foams:

Open celled metal foams are usually replicas using open-celled polyurethane foams as a skeleton and have a wide variety of applications including heat exchangers (compact electronics cooling, cryogen tanks, PCM heat exchangers), energy absorption, flow diffusion and lightweight optics. Due to the high cost of the material it is most typically used in advanced technology, aerospace, and manufacturing.

Extremely fine-scale open-cell foams, with cells too small to be visible to the naked eye, are used as high-temperature filters in the chemical industry.

Metallic foams are now-a-days used in the field of compact heat exchangers to increase heat transfer at the cost of an additional pressure drop.

However, their use permits to reduce substantially the physical size of a heat-exchanger, and so fabrication costs. To model these materials, most works uses idealized and periodic structures or averaged macroscopic properties.

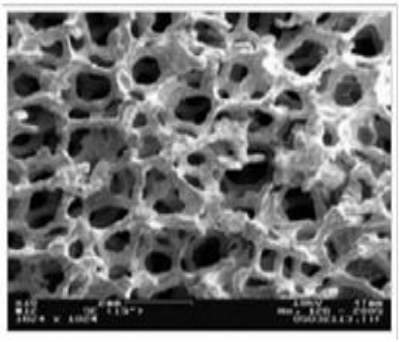

Figure 2.2 Open Cell Metal Foam

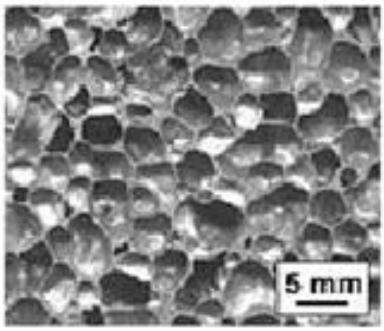

Figure 2.3.Closed-cell metal foam

2.2.2 Closed-cell metal foams:

Closed-cell metal foams are primarily used as an impact-absorbing material, similarly to the polymer foams in a bicycle helmet but for higher impact loads. Unlike many polymer foams, metal foams remain deformed after impact and can therefore only be used once. They are light (typically 10–25% of the density of an identical non-porous alloy; commonly those of Aluminium) and stiff, and are frequently proposed as a lightweight structural material. However, they have not yet been widely used for this purpose. Closed-cell foams retain the fire resistant and recycling capability of other metallic foams but add the ability to float in water.

A. Manufacturing Techniques of Metal Foams:

Literature survey revealed that metal foams can be produced by a variety of methods. The most common routes are via the addition of a foaming compound to molten metal or by passing air through molten metal. Such liquid metal processing routes generally produce relatively coarse structures. Powder routes, which result in foams with much finer structures, use mixtures containing gas-generating powders which react and release gases during processing. Other methods include the controlled sputtering of a metal with gas entrapment and liquid metal infiltration of packed spheres or granules. The structure and properties of the resulting materials are diverse. Literatures on various metal foam production is studied and a rough classification is presented in Figure 2.14.

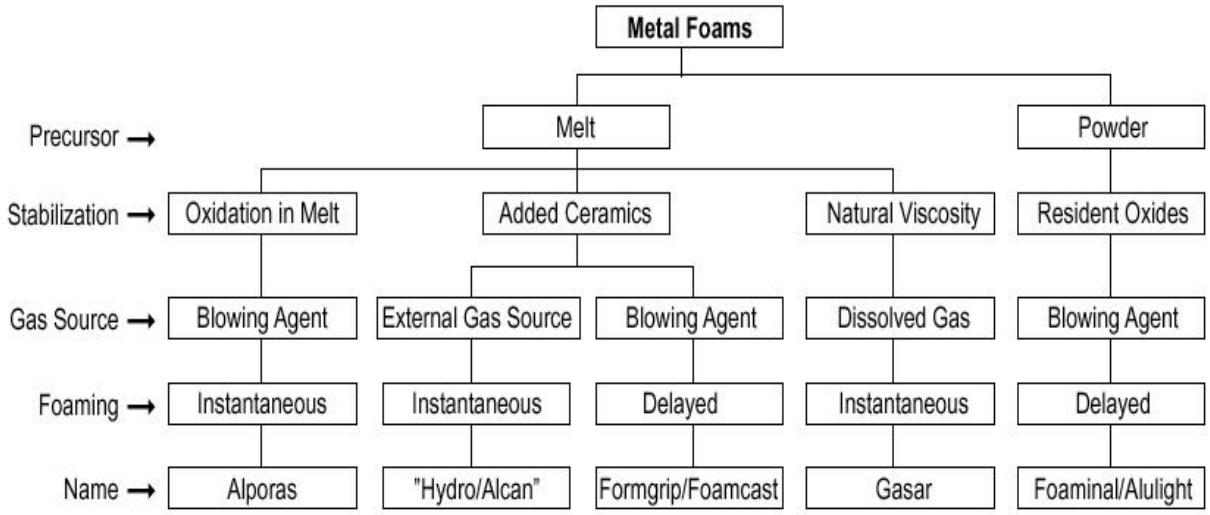

Fig. 2.14: Metal foam manufacturing routes

Precisely, nine distinct process-routes have been developed to make metal foams, of which five are now established commercially. They fall into four broad classes: those in which the foam is formed from the vapor phase; those in which the foam is electrodeposited from an aqueous solution; those which depend on liquid-state processing; and those in which the foam is created in the solid state. Each method can be used with a small subset of metals to create a porous material with a limited range of relative densities and cell sizes. Some produce open-cell foams,

others produce foams in which the majority of the cells are closed. The products differ greatly in quality and in price approximately can vary from $7 to $12 000 per kg.

2.4 Different techniques of making Metal Foams:

The properties of metal foam and other cellular metal structures depend upon the properties of the metal, the relative density and cell topology (e.g. open or closed cell, cell size, etc.). Metal foams are made by one of nine processes, listed below. Metals which have been foamed by a given process (or a variant of it) are listed in square brackets.[142]

1. Bubbling gas through molten Al – SiC or Al – Al2O3 alloys. [Al, Mg]

2. By stirring a foaming agent (typically TiH2) into a molten alloy (typically an aluminum alloy) and controlling the pressure while cooling. [Al]

3. Consolidation of a metal powder (aluminum alloys are the most common) with a particulate foaming agent (TiH2 again) followed by heating into the mushy state when the foaming agent releases hydrogen, expanding the material.[Al, Zn, Fe, Pb, Au]

4. Manufacture of a ceramic mold from a wax or polymer-foam precursor, followed by burning-out of the precursor and pressure infiltration with molten metal or metal powder slurry which is then sintered. [Al, Mg, Ni – Cr, stainless steel, Cu]

5. Vapor phase deposition or electro-deposition of metal onto a polymer foam precursor which is subsequently burned out, leaving cell edges with hollow cores. [Ni, Ti]

6. The trapping of high-pressure inert gas in pores by powder hot isostatic pressing (HIPing), followed by the expansion of the gas at elevated temperature. [Ti]

7. Sintering of hollow spheres, made by a modified atomization process, or from metal-oxide or hydride spheres followed by reduction or dehydridation, or by vapor-deposition of metal onto polymer spheres. [Ni, Co, Ni – Cr alloys]

8. Co-pressing of a metal powder with a leachable powder, or pressure-infiltration of a bed of leachable particles by a liquid metal, followed by leaching to leave a metal-foam skeleton. [Al, with salt as the leachable powder]

9. Dissolution of gas (typically, hydrogen) in a liquid metal under pressure, allowing it to be released in a controlled way during subsequent solidification. [Cu, Ni, Al]

Only the first five of these are in commercial production. Each method can be used with a small subset of metals to create a porous material with a limited range of relative densities and cell sizes. Figure 2.15 summarizes the ranges of cell size, cell type (open or closed), and relative densities that can be manufactured with current methods.

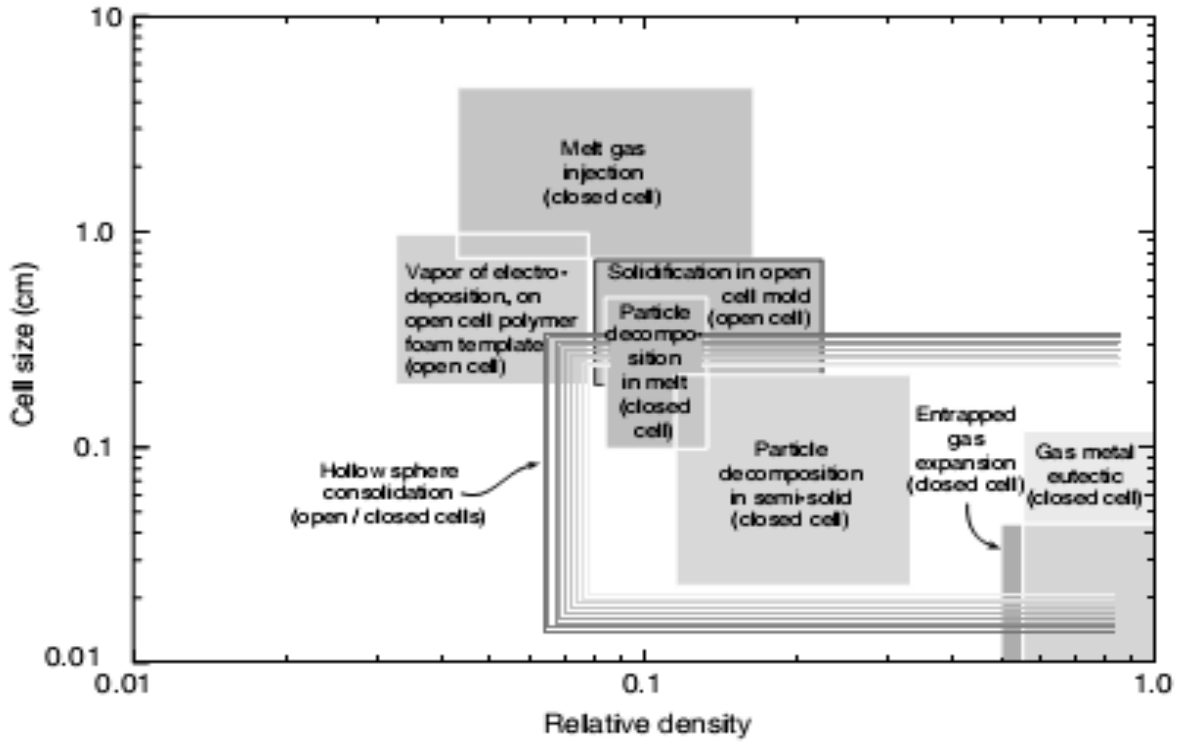

Fig. 2.15 The range of cell size and relative density for the different metal foam manufacturing methods

2.4.1 Melt gas injection (air bubbling):

Pure liquid metals cannot easily be caused to foam by bubbling a gas into them. Drainage of liquid down the walls of the bubbles usually occurs too quickly to create a foam that remains

stable long enough to solidify. However, 10 – 30% of small, insoluble, or slowly dissolving particles, such as aluminum oxide or silicon carbide, raises the viscosity of the aluminum melt and impedes drainage in the bubble membrane, stabilizing the foam. Gas-injection processes are easiest to implement with aluminum alloys because they have a low density and do not excessively oxidize when the melt is exposed to air or other gases containing oxygen. There are several variants of the method, one of which is shown in Figure 2.16. Pure aluminum or an aluminum alloy is melted and 5 – 15 wt% of the stabilizing ceramic particles are added. These particles, typically 0.5–25 μm in diameter, can be made of alumina, zirconia, silicon carbide, or titanium diboride.

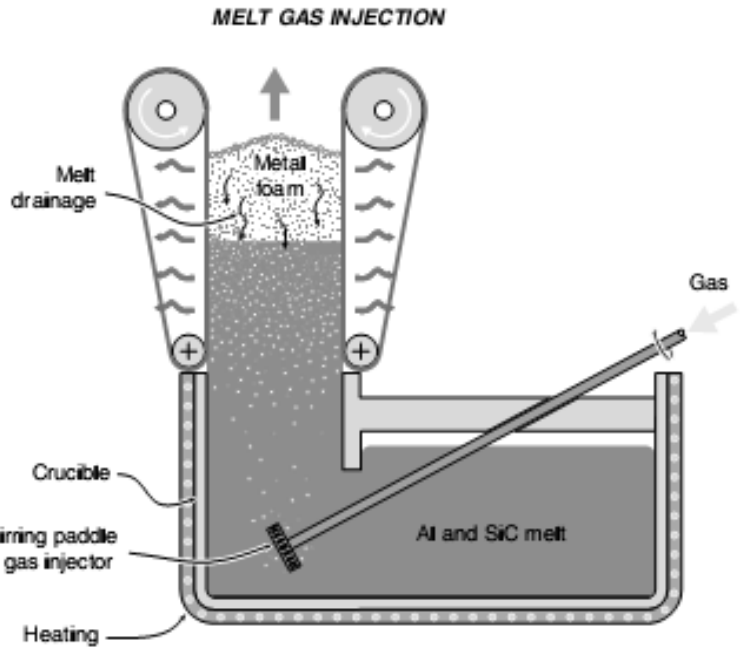

Figure 2.16 A schematic illustration of the manufacture of an aluminum foam by the melt gas injection method (CYMAT and HYDRO processes)

A variety of gases can be used to create bubbles within liquid aluminum. Air is most commonly used but carbon dioxide, oxygen, inert gases, and even water can also be injected into liquid aluminum to create bubbles. Bubbles formed by this process float to the melt surface, drain, and then begin to solidify. The thermal gradient in the foam determines how long the foam remains liquid or semi-solid, and thus the extent of drainage. Low relative density, closed-cell foams can be produced by carefully controlling the gas-injection process and the cooling rate of the foam.

Various techniques can be used to draw-off the foam and create large (up to 1 m wide and 0.2 m thick slabs containing closed cell pores with diameters between 5 and 20 mm. NORSK-HYDRO and CYMAT (the latter using a process developed by ALCAN in Canada) supply foamed aluminum alloys made this way. This approach is the least costly to implement and results in a foam with relative densities in the range 0.03 to 0.1. It is at present limited to the manufacture of aluminum foams.

2.4.2 Gas-releasing particle decomposition in the melt:

Metal alloys can be foamed by mixing into them a foaming agent that releases gas when heated. The widely used foaming agent titanium hydride (TiH2) begins to decompose into Ti and gaseous H2 when heated above about 465°C. By adding titanium hydride particles to aluminum melt, large volumes of hydrogen gas are rapidly produced, creating bubbles that can lead to closed-cell foam, provided foam drainage is sufficiently slow, which requires a high melt viscosity. The Shinko Wire Company has developed an aluminum foam trade named Alporas using this approach (Figure 2.17).

The process begins by melting aluminum and stabilizing the melt tempera-ture between 670 and 690°C. Its viscosity is then raised by adding 1 – 2% of calcium which rapidly oxidizes and forms finely dispersed CaO and CaAl2O4 particles. The melt is then aggressively stirred and 1 – 2% of TiH2 is added in the form of 5–20 μm diameter particles. As soon as these are dispersed in the melt, the stirring system is withdrawn, and foam is allowed to form above the melt. Control of the process is achieved by adjusting the overpressure, temperature and time. It takes, typically, about ten minutes to totally decompose the titanium hydride. When foaming is complete the melt is cooled to solidify the foam before the hydrogen escapes and the bubbles coalesce or collapse.

The volume fraction of calcium and titanium hydride added to the melt ultimately determines the relative density and, in combination with cooling conditions, the cell size. The cell size can be varied from 0.5 to 5 mm by changing the TiH2 content, and the foaming and cooling conditions. Relative densities from 0.2 to 0.07 can be obtained. As produced, the Alporas foam has predominantly closed cells, though a subsequent rolling treatment can be used to fracture many of the cell walls in order to increase their acoustic damping. A significant manufacturing capacity now exists in Japan. Although only small volume fractions of expensive Calcium and

Titanium hydride are used, the process is likely to be more costly than gas-injection methods because it is a batch process.

Today, only aluminum alloys are made in this way because hydrogen embrittles many metals and because the decomposition of TiH_2 occurs too quickly in higher melting point alloys. Research using alternative foaming agents (carbonates, nitrates) with higher decomposition temperatures offers the prospect of using this method to foam iron, steels and nickel-based alloys.

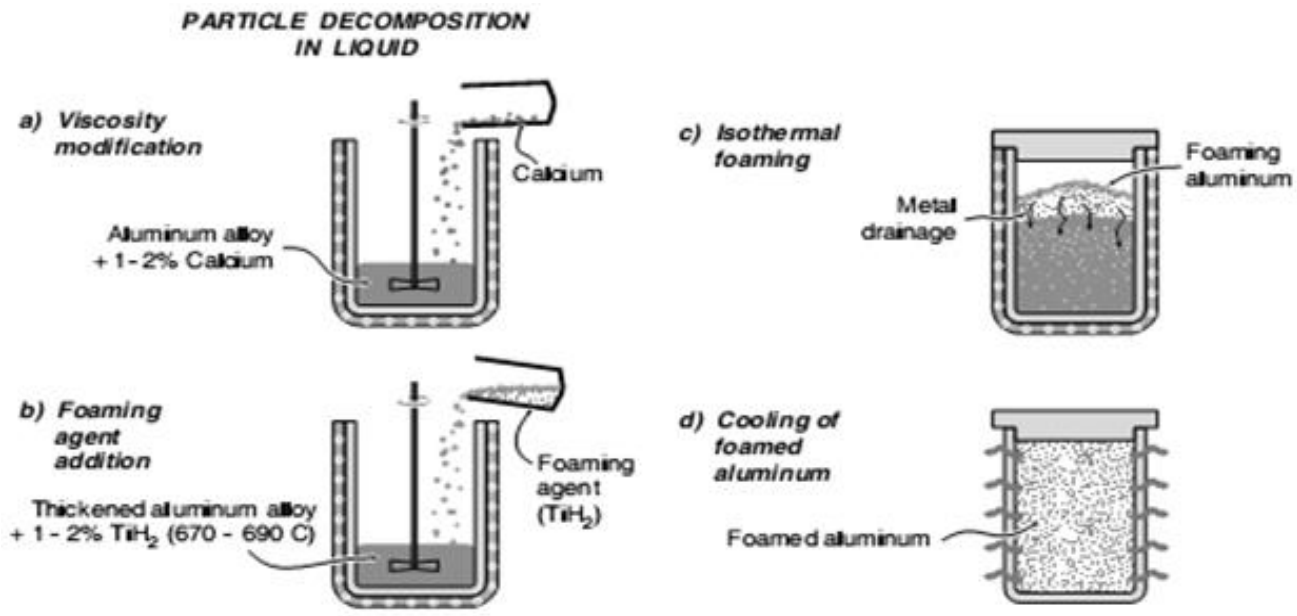

Figure 2.17 The process steps used in the manufacture of aluminum foams by gas-releasing particle decomposition in the melt (Alporas process)

2.4. 3 Gas-releasing particle decomposition in semi-solids:

Foaming agents can be introduced into metals in the solid state by mixing and consolidating powders. Titanium hydride, a widely used foaming agent, begins to decompose at about 465°C, which is well below the melting point of pure aluminum 660°C and of its alloys. This raises the possibility of creating foam by dispersing the foaming agent in solid aluminum using powder metallurgy processes and then raising the temperature sufficiently to cause gas release and partial or full melting of the metal, allowing bubble growth. Cooling then stabilizes the foam. Several

groups, notably IFAM in Bremen, Germany, LKR in Randshofen, Austria, and Neuman-Alu in Marktl, Austria, have developed this approach.

A schematic diagram of the manufacturing sequence is shown in Figure 2.29. It begins by combining particles of a foaming agent (typically titanium hydride) with an aluminum alloy powder. After the ingredients are thoroughly mixed, the powder is cold compacted and then extruded into a bar or plate of near theoretical density. This 'precursor' material is chopped into small pieces, placed inside a sealed split mold, and heated to a little above the solidus temperature of the alloy. The titanium hydride then decomposes, creating voids with a high internal pressure. These expand by semi-solid flow and the aluminum swells, creating foam that fills the mold. The process results in components with the same shape as the container and relative densities as low as 0.08. The foam has closed cells with diameters that range from 1 to 5 mm in diameter.

IFAM, Bremen, have developed a variant of the process, which has considerable potential for innovative structural use. Panel structures are made by first roll-bonding aluminum or steel face-sheets onto a core-sheet of unexpanded precursor. The unexpanded sandwich structure is then pressed or deep-drawn to shape and placed in a furnace to expand the core, gives a shaped, metal-foam cored sandwich-panel. Only foamed aluminum is commercially available today, but other alloy foams are being developed using different foaming agents.

2.4.4 Casting using a polymer or wax precursor as template:

Open-cell polymer foams with low relative densities and a wide range of cell sizes of great uniformity are available from numerous sources. They can be used as templates to create investment-casting molds into which a variety of metals and their alloys can be cast. It is thought that the ERG DUOCEL ranges of foams are made in this way. The method is schematically illustrated in Figure 2.18.

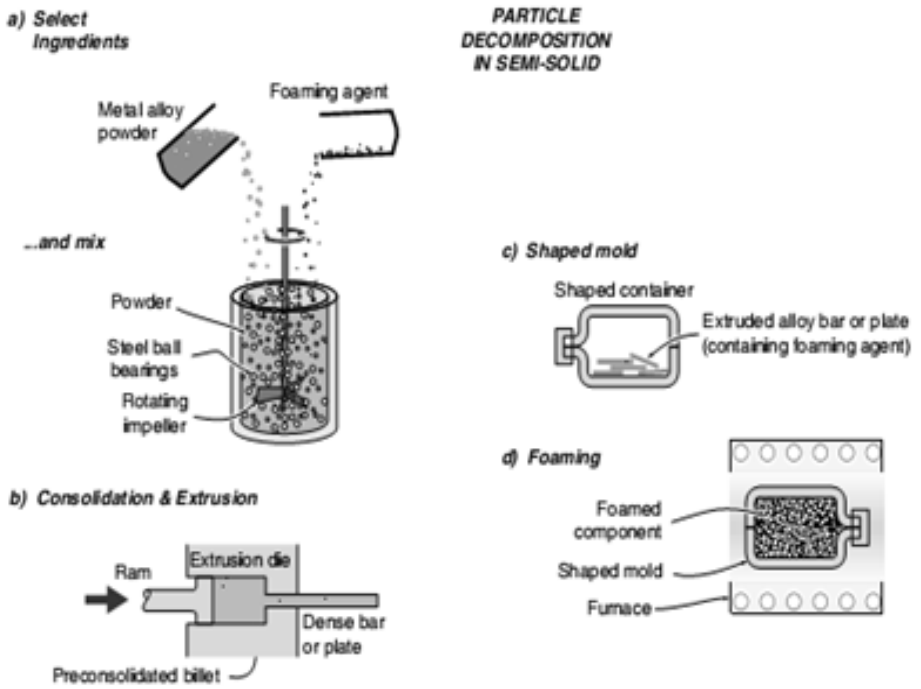

Figure 2.18 The sequence of powder metallurgy steps used to manufacture metal foams by gas-releasing particles in semi-solids (the Fraunhofer and the Alulight processes)

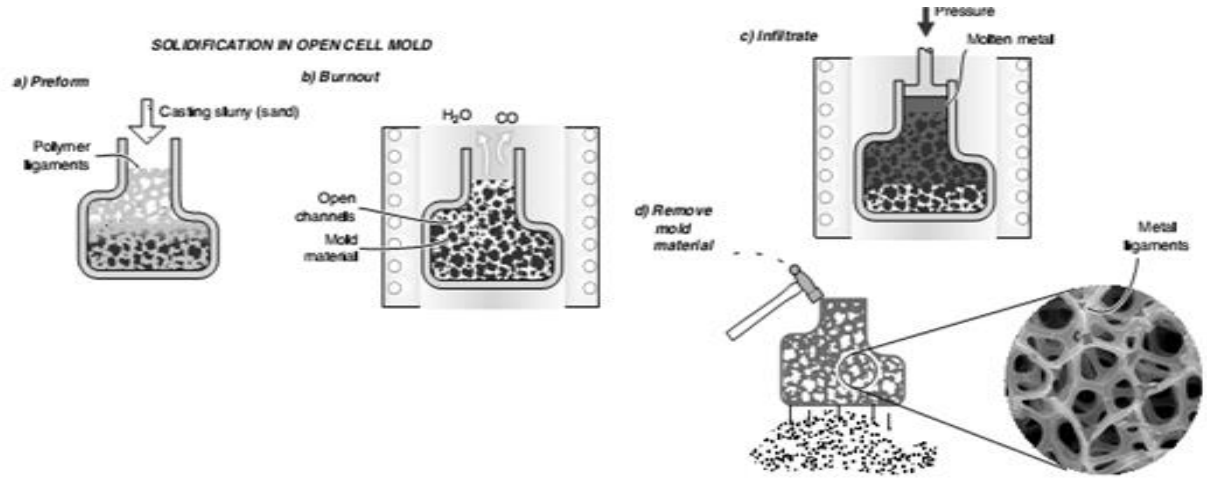

Figure 2.19: Investment casting method used to manufacture open cell foams (DUOCEL process)

An open-ll polymer foam mold template with the desired cell size and relative density is first selected. This can be coated with a mold casting (ceramic powder) slurry which is then dried and embedded in casting sand. The mold is then baked both to harden the casting material and to

decompose (and evaporate) the polymer template, leaving behind a negative image of the foam. This mold is subsequently filled with a metal alloy and allowed to cool. The use of a moderate pressure during melt infiltration can overcome the resistance to flow of some liquid alloys. After directional solidification and cooling, the mold materials are removed leaving behind the metal equivalent of the original polymer foam. Metal powder slurries can also be used instead of liquid metals. These are subsequently sintered. The method gives open-cell foams with pore sizes of 1 – 5 mm and relative densities as low as 0.05. The process can be used to manufacture foams from almost any metal that can be investment cast.

In a variant of the process, the precursor structure is assembled from injection-molded polymeric or wax lattices. The lattice structure is coated with casting slurry and fired, burning it out and leaving a negative image mold. Metal is cast or pressure-cast into the mold using conventional investment casting techniques.

2.4.5 Metal deposition on cellular preforms:

Open-cell polymer foams can serve as templates upon which metals are deposited by chemical vapor decomposition (CVD), by evaporation or by electro-deposition. In the INCO process, nickel is deposited by the decomposition of nickel carbonyl, $NiCO_4$. Figure 2.6 schematically illustrates one approach in which an open-cell polymer is placed in a CVD reactor and nickel carbonyl is introduced. This gas decomposes to nickel and carbon monoxide at a temperature of about 100°C and coats all the exposed heated surfaces within the reactor. Infrared or RF heating can be used to heat only the polymer foam. After several tens of micrometers of the metal have been deposited, the metal-coated polymer foam is removed from the CVD reactor and the polymer is burnt out by heating in air. This results in a cellular metal structure with hollow ligaments. A subsequent sintering step is used to densify the ligaments.

Nickel carbonyl gas is highly toxic and requires costly environmental controls before it can be used for manufacturing nickel foams. Some countries, such as the United States, have effectively banned its use and others make it prohibitively expensive to implement industrial processes that utilize nickel carbonyl gas. Electro- or electro-less deposition methods have also been used to coat the preforms, but the nickel deposited by the CVD technique has a lower electrical resistance than that created by other methods. The pore size can be varied over a wide range.

Foams with open pore sizes in the 100 – 300 μm diameter range are available. The method is restricted to pure elements such as nickel or titanium because of the difficulty of CVD or electro-deposition of alloys. It gives the lowest relative density (0.02 – 0.05) foams available today.

2.4.6 Entrapped gas expansion:

The solubility in metals of inert gases like argon is very low. Powder metallurgy techniques have been developed to manufacture materials with a dispersion of small pores containing an inert gas at a high pressure. When these materials are subsequently heated, the pore pressure increases and the pores expand by creep of the surrounding metal (Figure 2.20). This process has been used by Boeing to create low-density core (LDC) Ti – 6A1 – 4V sandwich panels with pore fractions up to 50%.

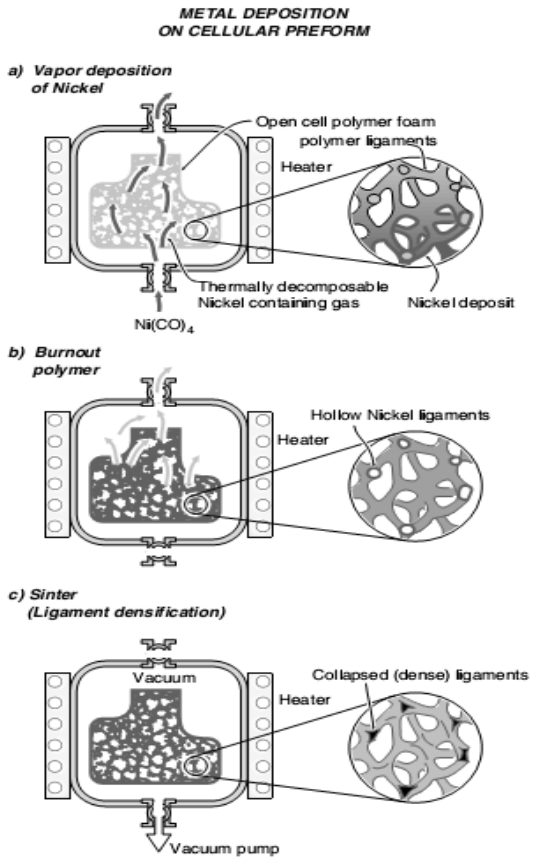

Figure 2.20 Schematic illustration of the CVD process used to create open-cell nickel foams (INCO process)

In the process Ti – 6A1 – 4V powder is sealed in a canister of the same alloy. The canister is evacuated to remove any oxygen (which embrittles titanium) and then backfilled with between 3 to 5 atmospheres (0.3–0.5MPa) of argon. The canister is then sealed and consolidated to a high relative density (0.9 – 0.98) by HIPing causing an eight-fold increase in void pressure. This is too low to cause expansion of Ti – 6AI – 4V at room temperature. The number of pores present in the consolidated sample is relatively low (it is comparable to the number of powder particles in the original compact), so a rolling step is introduced to refine the structure and create a more uniform distribution of small pores. In titanium alloys, rolling at 900 – 940°C, results in void flattening and elongation in the rolling direction. As the voids flatten, void faces come into contact and diffusion bond, creating strings of smaller gas-filled pores. Cross-rolling improves the uniformity of their distribution. Various cold sheet forming processes can then be used to shape the as-rolled plates.

The final step in the process sequence is expansion by heating at 900°C for 20 – 30 hours. The high temperature raises the internal pore pressure by the ratio of the absolute temperature of the furnace to that of the ambient (about a factor of four) i.e. to between 10 and 16 MPa, causing creep dilation and a reduction in the overall density of the sample.

This process results in shaped Ti-alloy sandwich construction components with a core containing a closed-cell void fraction of up to 0.5 and a void size of 10 – 300 μm. While it shares most of the same process steps as P/M manufacturing, and the cost of the inert gas is minor, HIPing and multipass hot cross-rolling of titanium can be expensive. This process is therefore likely to result in materials that are more costly to manufacture than P/M alloys.

2.4.7 Hollow sphere structures:

Several approaches have recently emerged for synthesizing hollow metal spheres. One exploits the observation that inert gas atomization often results in a small fraction (1 – 5%) of large-diameter (0.3 – 1 mm) hollow metal alloy spheres with relative densities as low as 0.1. These hollow particles can then be sorted by flotation methods, and consolidated by HIPing, by vacuum sintering, or by liquid-phase sintering. Liquid-phase sintering may be the preferred approach for some alloys since it avoids the compressive distortions of the thin-walled hollow powder particles that results from the HIPing process and avoids the prolonged high-temperature

treatments required to achieve strong particle – particle bonds by vacuum sintering methods. Porous nickel super-alloys and Ti – 6Al – 4V with relative densities of 0.06 can be produced in the laboratory using this approach. The development of controlled hollow powder atomization techniques may enable economical fabrication of low-density alloy structures via this route.

In an alternative method, hollow spheres are formed from slurry composed of a decomposable precursor such as TiH2, together with organic binders and solvents (Figure 2.21). The spheres are hardened by evaporation during their flight in a tall drop tower, heated to drive off the solvents and to volatilize the binder. A final heat treatment decomposes the metal hydride leaving hollow metal spheres. The approach, developed at Georgia Tech, can be applied to many materials, and is not limited to hydrides. As an example, an oxide mixture such as Fe2O3 plus Cr2O3 can be reduced to create stainless steel. In a third method developed at IFAM, Bremen, polystyrene spheres are coated with metal slurry and sintered, giving hollow metal spheres of high uniformity. The consolidation of hollow spheres gives a structure with a mixture of open and closed porosity. The ratio of the two types of porosity and the overall relative density can be tailored by varying the starting relative density of the hollow spheres and the extent of densification during consolidation. Overall relative densities as low as 0.05, are feasible with a pore size in the range from 100 μm to several millimeters.

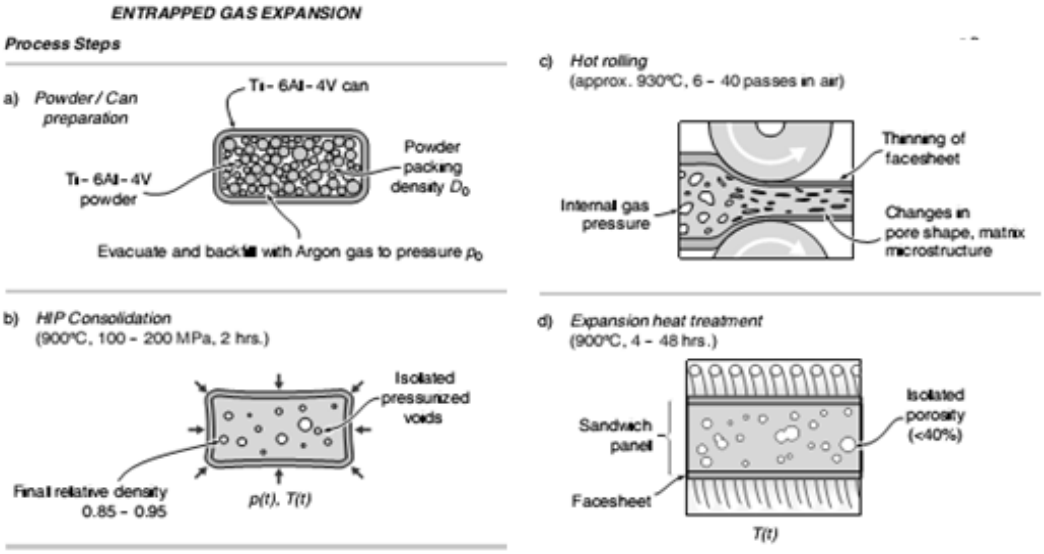

Figure 2.21 Process steps used to manufacture Titanium alloy sandwich panels with highly porous closed-cell with open- and closed-cell porosity

2.4.8 Co-compaction or casting of two materials, one leachable:

Two powders, with a volume fraction below 25%, are mixed and compacted, forming double-connected structures of both phases. After consolidation, one powder (e.g. salt) is leached out in a suitable solvent (Figure 2.22). Foams based on powder mixes of aluminum alloys with sodium chloride have successfully been made in large sections with uniform structures. The resulting cell shapes differ markedly from those of foams made by other methods. In practice the method is limited to producing materials with relative densities between 0.3 and 0.5. The cell size is determined by the powder particle size, and lies in the range 10 μm to 10 mm.

In an alternative but closely related process, a bed of particles of the leach-able material is infiltrated by liquid metal under pressure, and allowed to cool. Leaching of the particles again gives a cellular metallic structure of great uniformity.

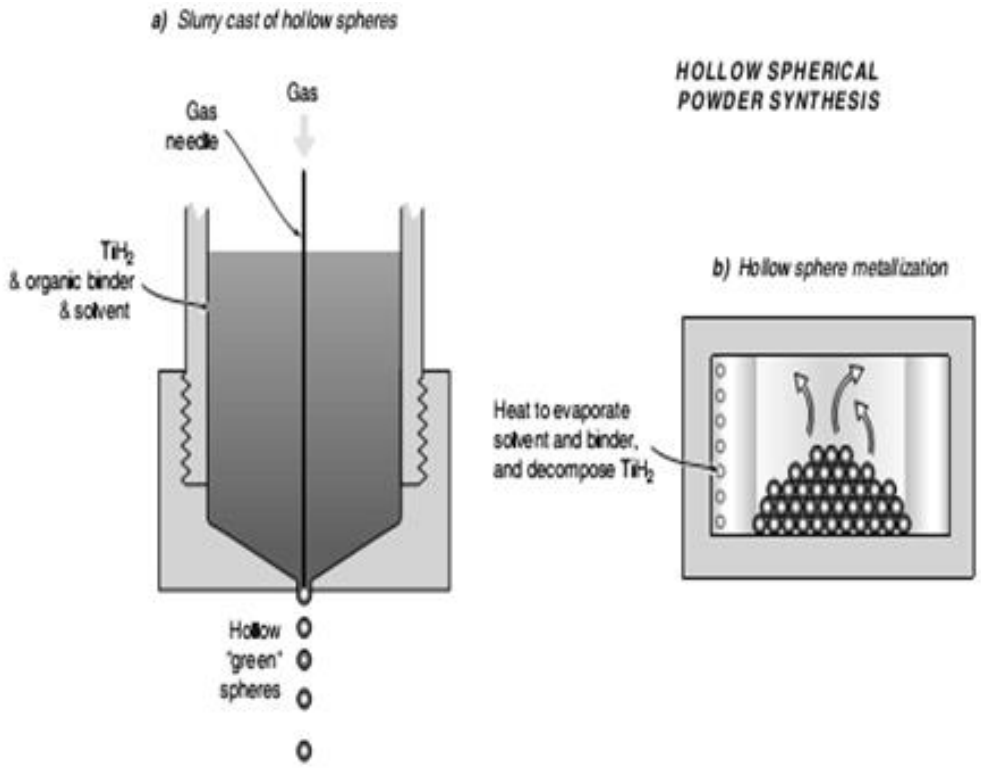

Figure 2.22 The Georgia Tech route for creating hollow metal spheres and their consolidation to create a foam cores

2.4.9 Gas–metal eutectic solidification:

Numerous metal alloy – hydrogen binary phase diagrams exhibit a eutectic; these include Al-, Be-, Cr-, Cu-, Fe-, Mg-, Mn- and Ni-based alloys. The alloys are melted, saturated with hydrogen under pressure, and then direction-ally solidified, progressively reducing the pressure. During solidification, solid metal and hydrogen simultaneously form by a gas eutectic reaction, resulting in a porous material containing hydrogen-filled pores. These materials are referred to as GASARs (or GASERITE).

A schematic diagram of the basic approach is shown in Figure 2.23. A furnace placed within a pressure vessel is used to melt an alloy under an appropriate pressure of hydrogen (typically 5 – 10 atmospheres of hydrogen). This melt is then poured into a mold where directional eutectic solidification is allowed to occur. This results in an object containing a reasonably large (up to 30%) volume fraction of pores. The pore volume fraction and pore orientation are a sensitive function of alloy chemistry, melt over-pressure, melt superheat (which affects the hydrogen solubility of the liquid metal), the temperature field in the liquid during solidification, and the rate of solidification. With so many process variables, control and optimization of the pore structure are difficult. The method poses certain safety issues, and in its present form is a batch process. As a result, materials manufactured by this route are costly. Though GASAR materials were among the first highly porous materials to attract significant interest, they remain confined to the laboratory and are not yet commercially available.

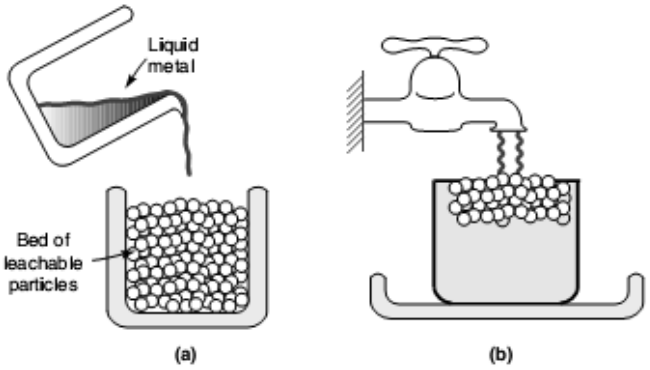

Figure 2.23 (a) A bed of leachable particles (such as salt), is infiltrated with a liquid metal (such as aluminum or one of its alloys). (b) The particles are dissolved in a suitable solvent (such as water) leaving an open-cell foam

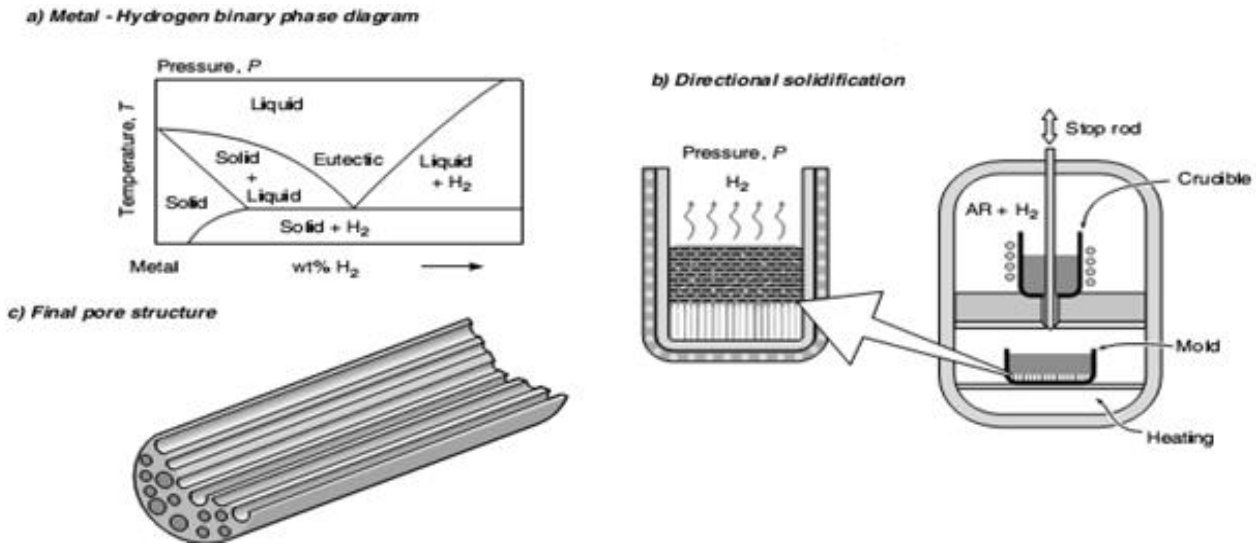

Figure 2.24 Gas–metal eutectic solidification for the manufacturing of GASARs

B. Characterization of Metal Foams

Relative density, foam morphology and pore size depend on the method of fabrication. These characteristics affect foam in physical and mechanical properties. Among these, relative density is the most important characteristic which affects mechanical properties of foams. Relative density is the ratio of foam density (ρ^*) to solid material density (ρ_s), i.e. ρ^*/ρ_s, and relates to porosity simply by ($1 - \rho^*/\rho_s$). Considering foam morphology, although cell shapes can vary substantially in variously fabricated foams, they are idealized as tetrakaidecahedral for theoretical analysis of foam deformation. In real foams, equi-axed cells produce isotropic material response and, conversely, elongated cells produce anisotropic material response. It is seen that the cells in open-cell foams produced through investment casting have a relatively uniform shape. Duocel®, is found to contain few morphological defects such as cracks in cell walls and cell wall wiggles. Closed-cell foams have varying cell shape and show significant morphological defects. In Fraunhofer foams major defects including cracks spanning 10 cells or more are also found [84]. Although there are exceptions pore size generally has little importance on most mechanical properties and is given in pores per inch (ppi) or pores per millimeter (ppm).

Some of the key physical properties of aluminum foam are those considered as thermal and electrical properties. It was already proved that in general foams have low thermal conductivities which are proportional to relative density. It was also found that the permeability to fluid flow of the foam varies with porosity and cell size, increasing as both foam parameters increase. The effect of porosity has the same impact on electrical conductivity of metal foams.

2.3.1 General Properties of Aluminium Foam:

General properties of aluminium metal foams are given below-

I. The defining characteristic of metal foams is a very high porosity: typically 75–95% of the volume consists of void spaces.

II. The strength of foamed metal possesses a power law relationship to its density; i.e., a 20% dense material is more than twice as strong as 10% dense material.

III. Metallic foams typically retain some physical properties of their base material. Such as, Foam made from non-flammable metal will remain non-flammable; Coefficient of thermal expansion will also remain similar as the base material while thermal conductivity will likely to be reduced than solid of same volume.

IV. They are light (typically 10–25% of the density of an identical non-porous alloy; commonly those of aluminium) and stiff, and are frequently proposed as a lightweight structural material.

V. After maximum compression it acts like a solid made of same material. Foam properties get disappeared.

VI. Closed cell foams made from aluminium have the ability to float in water.

VII. Normally the closed cell foams are fire resistant.

VIII. High energy absorption ability.

2.3.2 Mechanical Properties of Aluminium Foams:

Under uni-axial compressive loads, Al closed cell foams show characteristic compressive stress strain behavior. The ideal compressive stress strain curve comprises three distinct deformation regions (Figure 2.4). In linear elastic region, the foam deformation is controlled by cell edge bending and/or cell face stretching. Collapse region occurs by highly localized cell edge buckling, crushing and tearing (Figure 2.5). The collapse region is characterized by a collapse stress and/or a plateau stress either with a constant value or increasing slightly with strain (Figure 2.4). At a critical strain, ε_d, the cell walls start to touch each other and, as a result of this, the material densifies. The stress in this region increases sharply and approaches to the strength of the bulk Al metal.

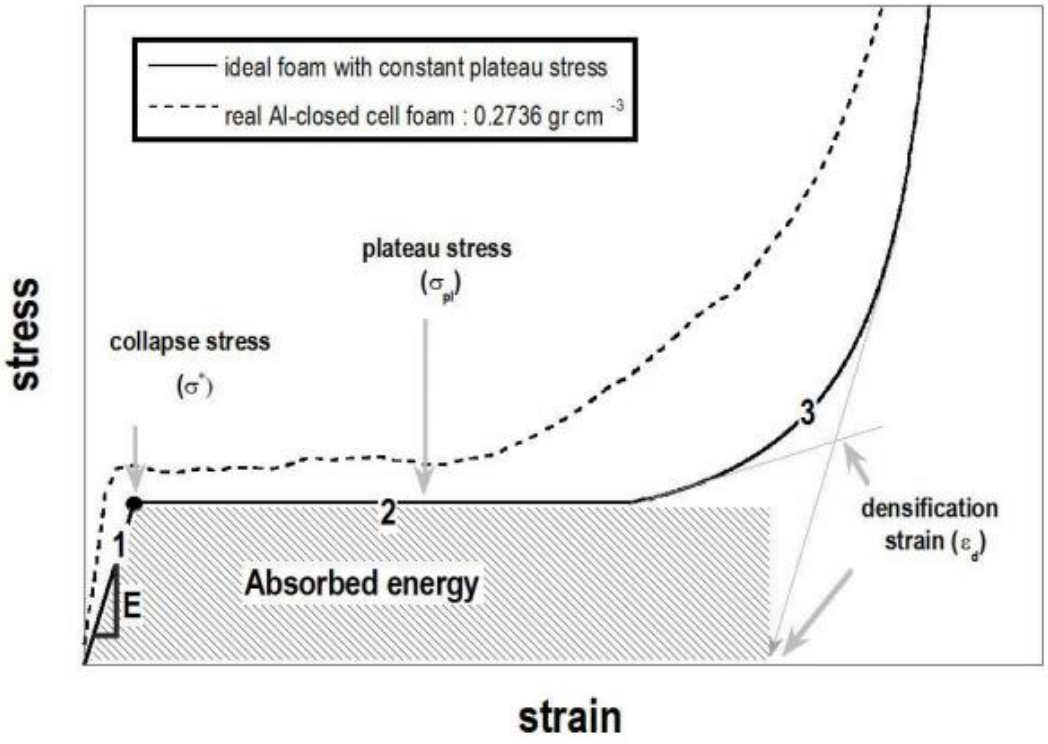

Figure 2.4 Compression stress strain curves of ideal foam and real Al-closed cell foam.

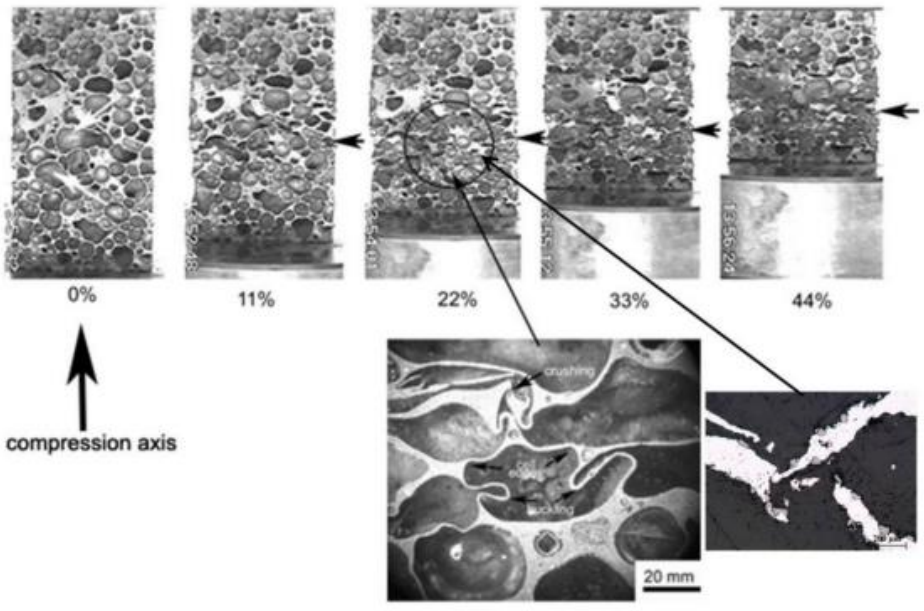

Figure 2.5 The deformation of highly localized Al foam sample at different strains and deformed foam cell structure in the localized deformed region. [97]

The elastic modulus (E*) of ideal open and closed cell foams are calculated from the cell edge bending deflection and the stretching of the planar cell faces and is given sequentially as [1],

$$\frac{E^*}{E_s} = c_1\rho^2 \tag{2.1}$$

$$\frac{E^*}{E_s} = c_2\rho^2 + c_3\rho \approx c_4\rho \tag{2.2}$$

where, Es is the elastic modulus of the cell wall material, c_1 , c_2 , c_3 and c_4 are the constants and ρ is the foam relative density (RD) which is

$$\rho = \frac{\rho^*}{\rho_s} \tag{2.3}$$

Where, ρ* is the density of foam and ρ_s is the density of the cell wall material. For tetrakaidecahedral foams, $c_1 \approx 1$, $c_2 = c_3 \approx 0.32$ and for low density foams, $c4 \approx 0.32$. The experimentally measured elastic moduli data in Figure [2.6(a)] are shown to present relatively good correlations with the open cell foam modulus values predicted by the Equations 2.1 and 2.2 [96].

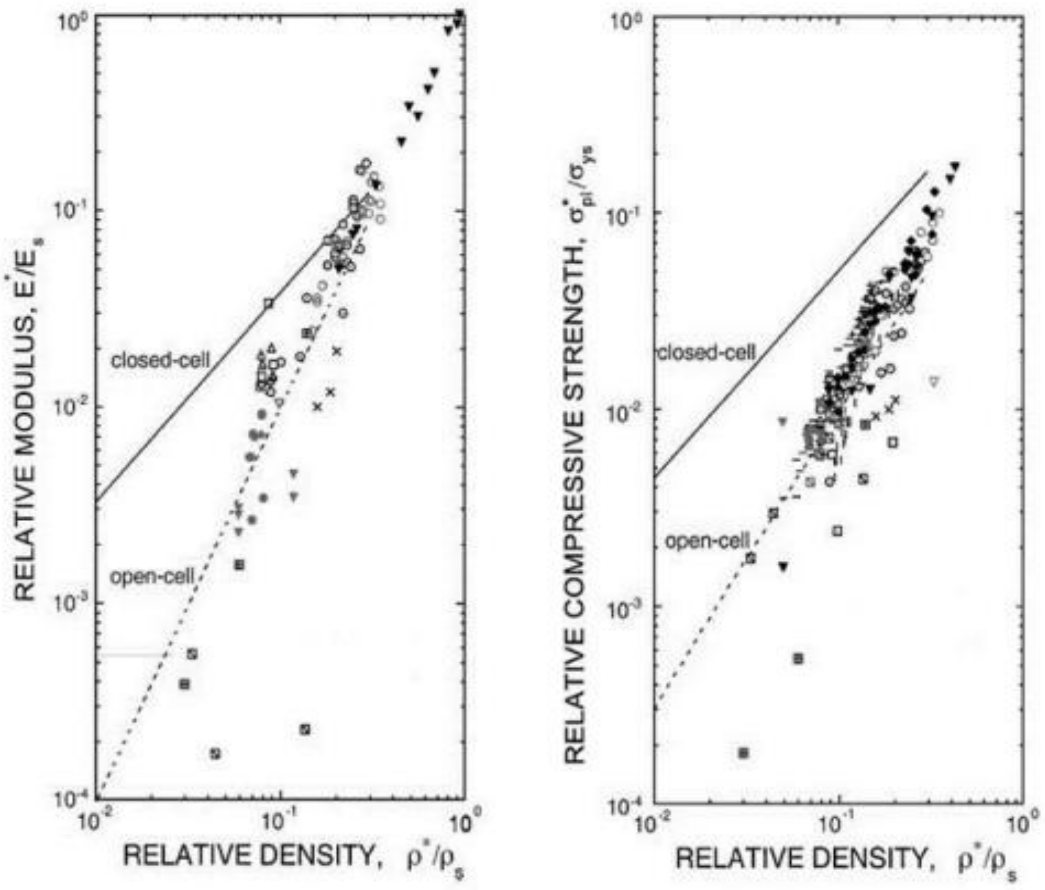

Figure 2.6 (a) Relative modulus vs. relative density and, (b) relative compressive strength vs. relative density graphics of open and closed cell Al foam.

The plateau stress determines the amount and efficiency of the energy absorption in the collapse region. For ideal open and close cell foams, the plastic collapse simply occurs by the plastic hinges at the bend cell edges and the cell wall stretching in perpendicular direction to the compression axis. Equations 2.4 and 2.5 relate sequentially the plateau stresses of ideal open-cell and tetrakaidecahedral closed-cell foams with relative density as,

$$\frac{\sigma_{pl}}{\sigma_{ys}} = 0.3\rho^{3/2} \qquad (2.4)$$

$$\frac{\sigma_{pl}}{\sigma_{ys}} = 0.33\rho^{2} + 0.44\rho \qquad (2.5)$$

Where, σ_{pl} is the plateau stress and σ_{ys} is the yield strength of the cell wall material. Relatively good correlations between the experimental relative compressive strength values of open and closed cell foams with compressive strength values predicted using Equation 2.4, which was developed for the open cell foams, was shown previously (Figure 2.6(b)). While, the experimental closed cell Al foam strength values showed deviations from the ideal strength data as depicted in Figure 2.6(b). This was attributed to the micro structural defects formed during manufacturing the closed cell foams including missing, fractured and bent cell walls and inhomogeneous cell wall allocations between cell walls and cell edges. The defects may produce premature bending leading to the initiation of a deformation band in the foam.

2.3.3 Stress-Strain Behaviour under Compression:

To understand the stress-strain behavior, a simple cubic unit cell model is developed to predict many normalized mechanical properties of foam structures. The cubic unit cell depicting closed-cell foam can be seen in Figure 2.7. Where the foaming is occurred along T direction, the stress-strain curves are provided in Figure 2.8.

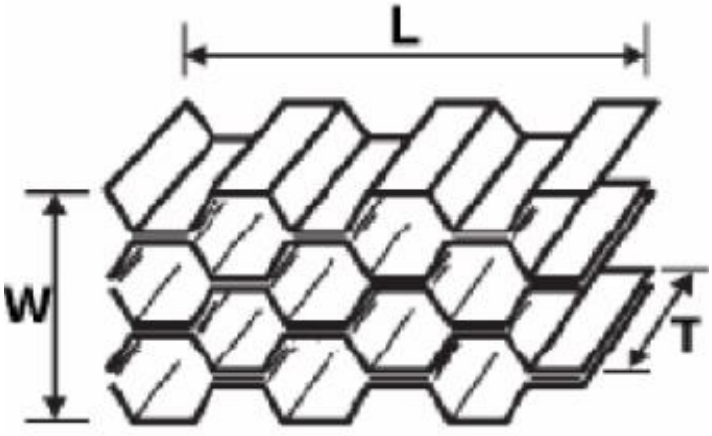

Figure 2.7 closed cell foam of dimension w x l x t

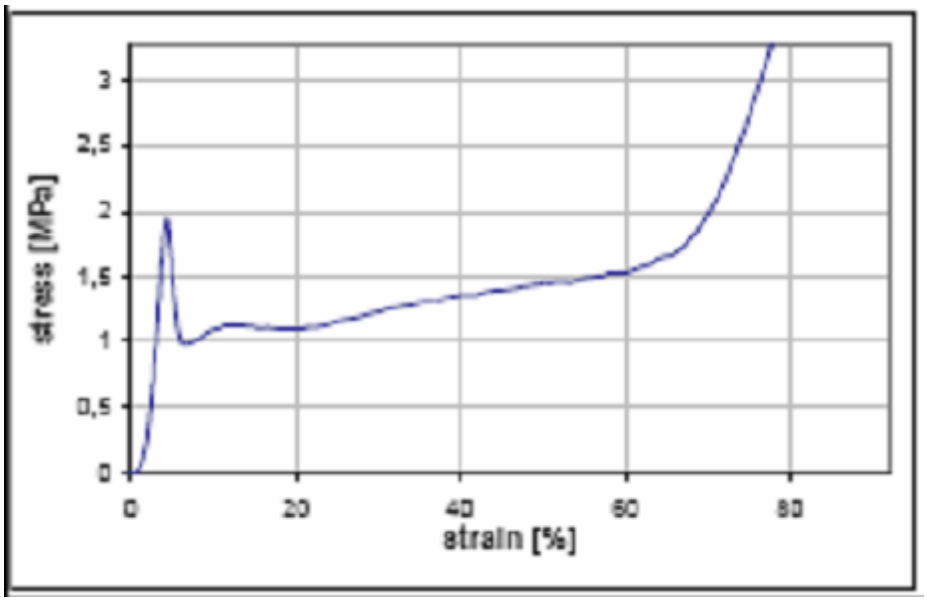

Figure 2.8 (a) Stress-Strain behavior along T direction under compression

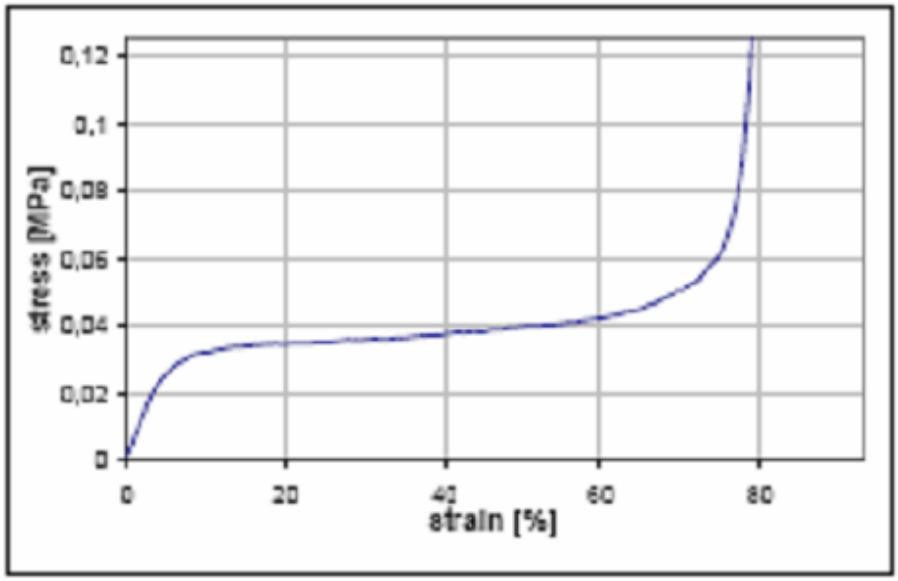

Figure 2.8 (b) Stress-Strain behavior along L direction under compression

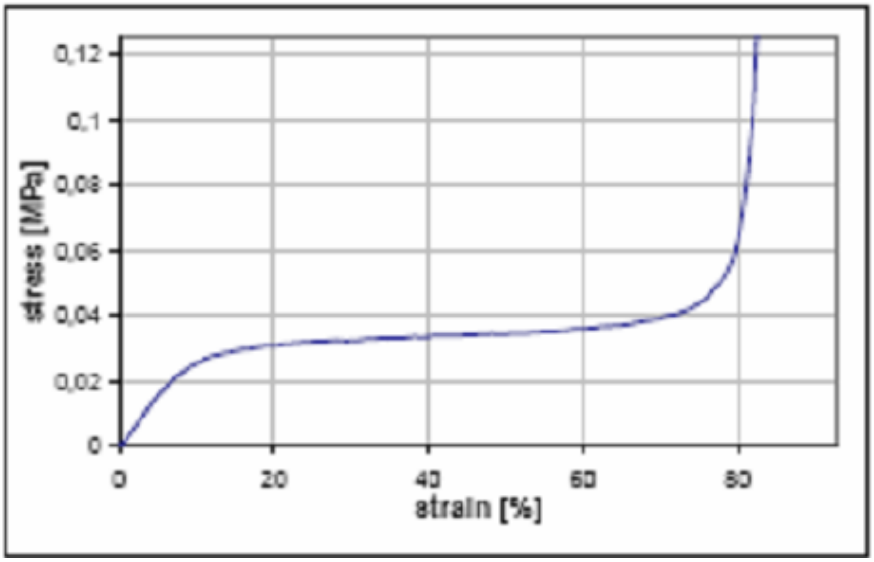

Figure 2.8 (c) Stress-Strain behaviors along w direction under compression

. In the model, the cell has a side length l and a square wall cross section of thickness t. The purpose of the model is to yield scaled relationships based on bulk material properties and relative density. The relative density of the unit cell is given by:

$$\frac{\rho^*}{\rho_s} \propto \left(\frac{t}{l}\right)^2 \tag{2.6}$$

Compressive deformation of aluminum foam produces a distinctive type of stress-strain curves. Important mechanical properties including the elastic modulus, yield and plateau strengths are obtained from these curves. Figure 2.5 (a) shows a schematic of a typical aluminum foam stress-strain curve displaying the three regions characteristic of plastic foam. Region I is linear-elastic followed by a plastic collapse plateau in Region II. Region II is truncated by densification of the foam in Region III. The stress-strain curve for brittle foams has a similar shape and contains the same three regions. However, a significant stress peak is observed at the end of Region I and Region II is rough with many stress peaks and valleys shown in Figure 2.9 (b).

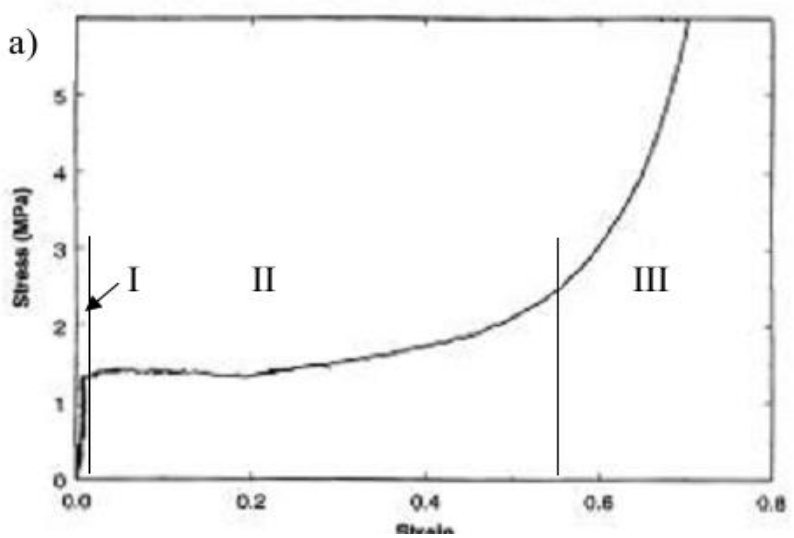

Figure 2.9 (a) A typical stress-strain curve for a plastic open-cell aluminum foam[84] and a schematic presentation of various deformation regimes.

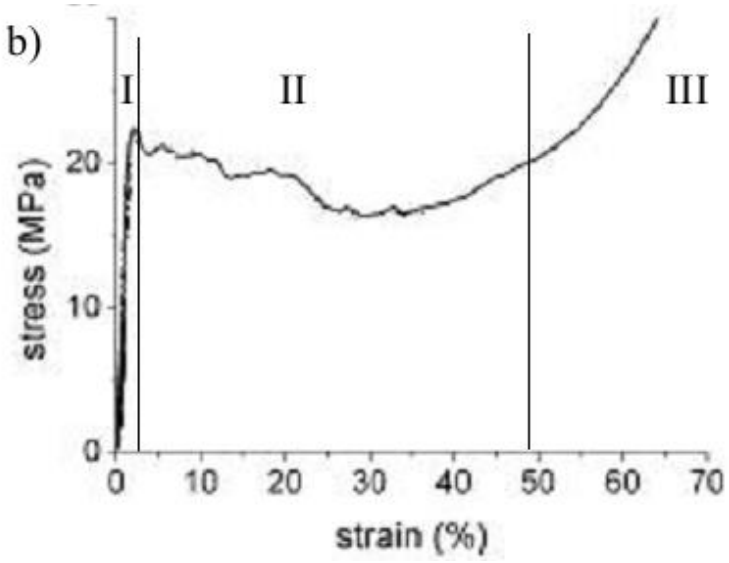

2.9 (b) A typical stress-strain curve for brittle aluminum foam and a schematic presentation of various deformation regimes**.**

Region I is then broken down further into two sub regions. Figure 2.10 shows the two sub regions on a log-log plot. Region Ia is purely elastic while Region Ib is elasto-plastic showing micro-plastic deformation. The initial linear-elastic behaviour of aluminum foam is dependent on relative density. For open-cell foams the initial linear-elastic deformation produces a

heterogeneous strain distribution and is controlled by cell wall bending. In the region beyond linear-elasticity but before yielding (or Region Ib) no visible permanent deformation is observed, however dislocation slip bands can be seen on the surface of some of the struts under scanning electron microscopy SEM). Plastic collapse of cell walls occurs when the moment exerted on the cell edges is higher than their plastic moment leading to the formation of plastic hinges and subsequent cell wall buckling and signals the end of Region I and the beginning of Region II. The plastic collapse strength occurring at the beginning of Region II is taken as the foam yield strength (Ϭ*) by some researchers.

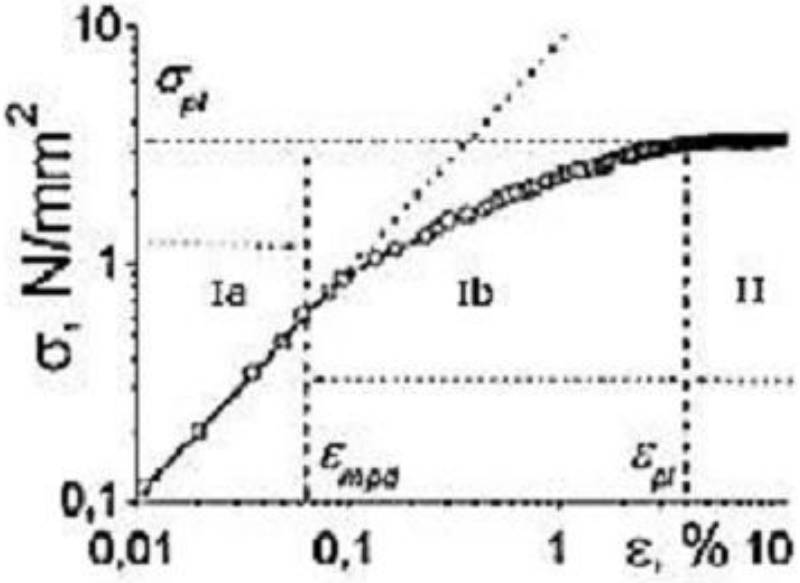

Figure 2.10 The subdivision of Region I in to a linear elastic region (i.e. Region Ia) and an elasto-plastic region (i.e. Region Ib)

The yield stress is defined as the maximum observed stress up to a strain of 0.05. In reality a steady increase in stress due to hardening of the cell wall material is observed, although the stress may initially drop slightly from Ϭ *. The foam crushes in discrete bands in which the localized strain is greater than the macroscopic strain level.

At the end of Region II the collapse and deformation of cell walls becomes significant enough that the walls begin to touch, i.e. densification begins. Region III is characterized by the densification process of the foam where by porosity is removed. However the removal of all

porosity from the foam during a compression test is difficult and rarely achieved. The densified foam behaves as a solid material requiring large stresses for further compression. Foam densification occurs at the densification Strain e_d. The point at which the foam densifies is not well defined and the definition is found to vary between researchers. Common methods of determining the densification strain (or stress) based on the stress-strain response are by visual inspection, at a stress 1.5 times the stress value at a strain of 0.5. The former method utilizes the point of intersection of the slope of the plateau region and that of the densification region as the point of densification. This is can be inaccurate as the slope of the plateau can be suppressed by increasing the scale on the stress axis thus changing the point of densification. The latter method is better as the point of densification remains constant regardless of the choice of scale, however as noted by the authors this method is arbitrary. Other researchers' choose an arbitrary strain and utilize this as the densification point. In structural applications the densification point is not as important as the yield point. However in energy absorption applications the point of densification is important and compression beyond densification is to be avoided due to the sharp increase in stress. The Cushion factor (C) is the ratio of peak stress to energy absorbed. It was established that the maximum useful displacement (d_{max}) occurs at the point of maximum Total Efficiency (T_E). Where T_E is approximately equivalent to 1/C. using this definition, the densification stress is taken as the shoulder of the energy absorption curve (i.e. the point of highest energy absorbed to peak stress). Although ideally these are the same points, reading the shoulder point from the graph can give different results depending on what scale for the axis is chosen.

2.3.4 Stress-Strain Behaviour under Static Compression Testing:

The stress-strain curves of closed-cell foams display either plastic or brittle fracture depending on foam fabrication and microstructure. Variations in porosity of closed-cell foams result in heterogeneous elastic modulus and yield strength values throughout the specimen. Many researchers have noted the low experimental values of elastic modulus and yield strength compared to the values predicted by the mechanical models developed for closed cell foams. This is attributed to stress concentrations occurring at the nodes and morphological defects in the foam such as curvature in the cell edges and cracks. As with open-cell foams, higher relative densities shorten the plateau.

2.3.5 Energy Absorption under Compression:

The long stress plateau typical of the stress-strain curves of aluminum foams gives rise to excellent energy absorption properties. Damage to an object is caused when a critical force (or acceleration) level is exceeded. The ability to absorb energy at a force below this critical level is paramount to the protection of the object. The force of an impact is directly related through geometry to the stress in the foam. Figure 2.13 shows why foams are much better than solid materials at providing damage protection. For a given stress foams always absorb more energy than a solid due to the bending, buckling and fracture of the foam cell walls. The following section is based on the analysis of energy absorption properties of cellular materials. The compression of aluminum foam under an applied force results in work. The work per unit volume (W) up to a strain of e is the area under the stress-strain curve. It is calculated in the following manner

$$W = \int_0^e \sigma(e)de \qquad (2.7)$$

Little energy absorption occurs in the initial linear elastic region. Energy absorption in the plateau region accounts for the majority of energy absorbed by the specimen. Plastic deformation of Aluminum foams at near constant stress in the plateau region translates into energy dissipated at near constant stress. Ideally for better energy absorption the stress-strain curve would be perfectly horizontal from e = 0 to e_d. After densification modest increase in energy absorption is accompanied by large stress increases.

Considering impact conditions (i.e. strain rates in the range of 10^1 to $10^4 s^{-1}$), there is an optimum foam density to absorb energy efficiently. This is illustrated in Figure 2.12 where three foams of different relative densities are shown schematically. The stress and strain at which an amount of energy W is absorbed is shown for all three densities. This shows that if too weak of a material is chosen the required amount of energy absorbed is more than that under the plateau, the foam densifies and the force increases sharply before all energy is absorbed. If however too strong of a material is chosen the load becomes too large before all the required energy is absorbed. The most efficient foam is shown to have the middle density. Here the full plateau is employed in

energy absorption while $e < e_d$ and the load transferred to the object is minimized (i. e. $(\sigma_p)_2 < (\sigma_p)_1$ and $(\sigma_p)_3$ where σ_p represents the peak, i.e. highest recorded stress for the chosen value W calculated from 0 strain)

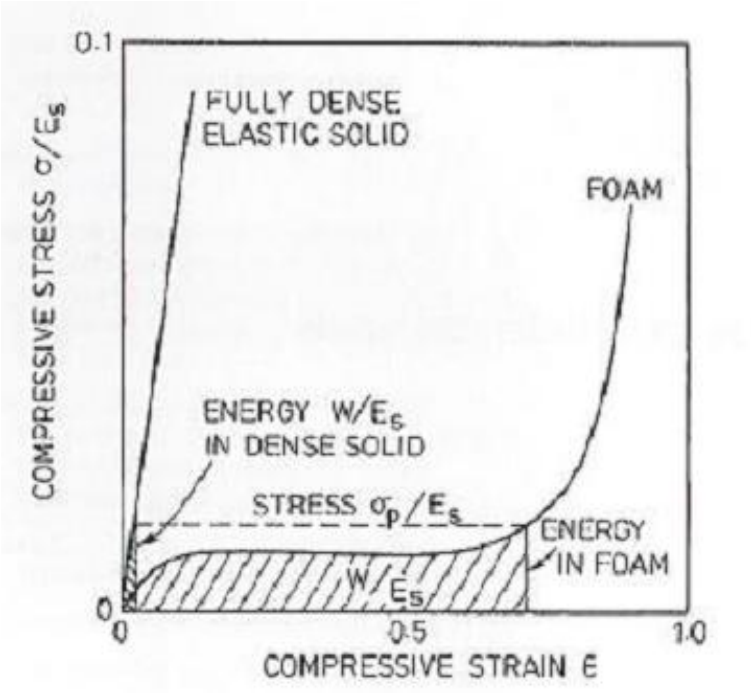

Figure 2.11 Stress-strain curves for both an elastic solid and foam showing the difference in energy per unit volume absorbed at the same stress level.

Figure 2.12 shows energy absorption (W) vs. σ_p curves of ideal open-cell plastic foams at various relative densities, at a constant strain rate. It should be emphasized that the curves are plotted using log scale on both axes and both W and σ_p are normalized by the bulk material elastic modulus (E_s). The initial parts of the curves display the energy absorbed in the linear-elastic regime. The plateau regime is responsible for the vertical slope displaying large increases in energy absorption with no increase in stress. In real foams, however, the plateau is not horizontal and therefore the slope in this region of the energy absorption curve deviates slightly from the vertical trend, showing a reduction in slope. At the end of this region (i. e. when the vertical part of the curve changes to horizontal) a shoulder in the energy absorption curve is observed. The shoulder occurs at the foam densification stress σ_d (i.e. the stress at which σ_d occurs). The horizontal slope following the shoulder is due to the densification of the foam. This is for idealized foams; in real foams this slope is greater than zero.

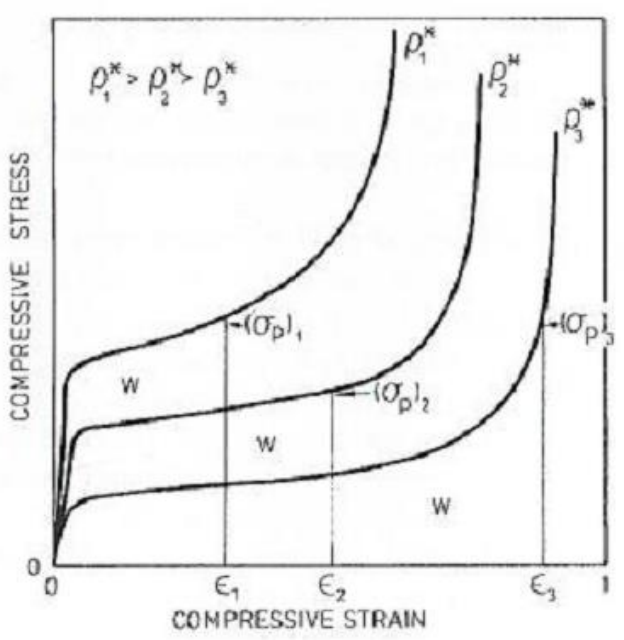

Figure 2.12: Schematic of three different relative density stress-strain curves. The curves show the stress levels for the equal energy absorption (W) for each case. The middle foam absorbs The amount of energy W at the lowest peak stress $(\sigma_p)_2$.

Two methods of comparing and choosing foams for energy absorption applications will be reviewed. The first method involves comparing the energy absorption efficiency of the different materials. There is a range of methods that determine the efficiency of energy absorption. One such method is stated below. Here the efficiency (ξ) up to a strain e is determined as

$$\xi(e) = \frac{\int_0^e \sigma(e)de}{\sigma_p e} \qquad (2.8)$$

The numerator is simply W, while the denominator represents the energy absorbed by an ideally horizontal stress-strain curve. This method is only beneficial when comparing materials at the same strain and does not correlate well to maximum energy absorbed at a maximum allowable load. Another measure of efficiency is the Cushion factor. The Cushion factor relates the amount of energy absorbed to peak stress. It is determined in the following manner

$$C = \frac{\sigma_p}{W} \qquad (2.9)$$

The lower the value of C the more energy a foam can absorb in relation to its peak stress and the more efficient it is considered. This relation is important as it correlates directly to the level of energy to be absorbed and the allowable load limit of impacts. The Cushion factor also takes into account both deviations from the ideal stress-strain curve for energy absorption (i.e. horizontal stress-strain curve) and the amount of strain up to densification. In this investigation when two materials have similar densification stresses a comparison of the Cushion factors will be used to determine the most appropriate material for energy absorption applications.

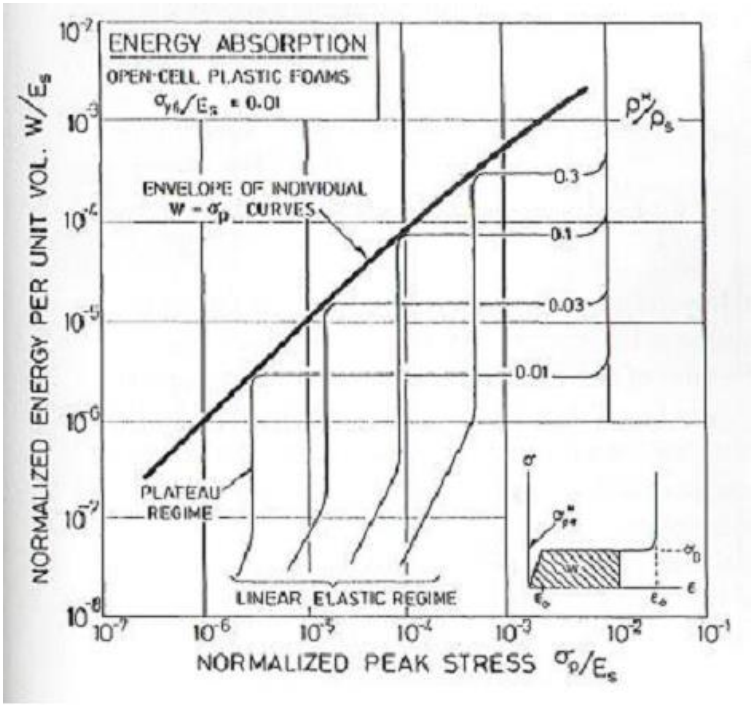

Figure 2.13: Energy absorption curves for ideal open-cell plastic foams at a constant strain rate for various relative densities.

A second method for choosing a suitable material for energy absorption applications are the energy absorption curves. This method is well suited for comparing materials which have different densification stresses. The most suitable material is the one that absorbs the most energy at the maximum allowable stress of impact. Ideally the densification stress of the material (or shoulder of the energy absorption curve) is the same as the maximum allowable stress. This

method will also be utilized in this investigation when comparing two materials with different densification stresses.

2.3.5 Energy Absorption under Static Compression Testing:

Energy absorption is affected by the shape of the stress-strain curve. The increase in plateau stresses due to increased relative densities result in higher values of energy absorbed However, the energy absorption efficiency as defined by equation (2.8) is unaffected by relative density but changes with loading direction in anisotropic foams. The defects in closed cell foams decrease the energy absorption efficiency. By careful control of foam production, it is possible to produce closed-cell Alporas® with small cell sizes, reduced density gradients, cell wall curvature and corrugation. The modified foam with fewer defects not only shows an increase in energy absorption over the unmodified foam with similar relative density, it also displays an increase in energy absorption efficiency.

Mechanical Damping Capacity Studies:

Few materials behave in a perfectly elastic manner regardless of stress level. This inelasticity results in the dissipation of energy (or damping) and is due to internal friction mechanisms within the specimen. Relevant damping mechanisms to aluminum foams are reviewed by various researchers. This will be followed by the stress-strain behaviour of closed-cell aluminum foams under cyclic loading and the damping properties (i. e. energy absorption) of closed-cell aluminum foams due to the lack of literature on damping of open-cell aluminum foams.

Mechanical Damping Mechanisms:

Mechanical damping is caused by internal friction mechanisms. These mechanisms can be classified as linear (i.e. strain/stress amplitude independent) or non-linear (i.e. strain/stress amplitude dependent) and are generally related to the movement of atoms and defects. The two major relevant mechanisms of linear internal friction are thermo-elastic effects (or thermal gradients) and dislocation damping. Thermo-elastic effects produce damping due to elastic stress gradients in non-uniformly stressed specimens. The elastic stress gradients set up temperature gradients which in turn lead to thermal currents, dissipating energy as heat. Damping due to thermo-elastic effects reaches a maximum at a resonant frequency that is dependent on the well

defined bulk specimen thickness. The damping capacity quickly drops as the difference between testing frequency and resonant frequency increases. An accepted model of dislocation damping is the vibrating string dislocation model proposed by **Koehler** and modified by **Granato and Lücke**. In the model, at low strain/stress amplitudes the dislocations bow out between pinning points, dissipating energy as heat. The amount of energy dissipated is frequency dependant. Relevant non-linear internal friction mechanisms include an extension of the vibrating string dislocation model and energy dissipation due to plastic strain. In the vibrating string dislocation model, if the strain/stress amplitude is sufficiently high the dislocations breakaway from the pinning points. Upon reversal of stress the dislocation contracts via a different path producing a hysteresis loop. Non-linear dislocation damping dissipates more energy than linear dislocation damping. At stress amplitudes between the elastic limit and the true fracture strength of the material new dislocations are produced and the dissipation of energy is due predominantly to plastic strain. Cyclic loading in this range is unstable as fatigue of the material eventually occurs.

Typically the internal friction mechanisms responsible for damping in bulk metals also results in damping in their respective cellular materials. However, the highly heterogeneous structure of cellular materials alters how these mechanisms occur and results in some new internal friction mechanisms. For damping due to thermo-elastic effects, the cellular structure of foams disrupts the flow of the thermal gradients resulting in a distribution of apparent thickness values. Therefore there is a large range of apparent resonant frequencies which produces damping compared to the smaller frequency range seen in the bulk material. Little change occurs in the mechanism of dislocation damping. The higher localized strains/stresses produced by localized deformation means that amplitude dependant dislocation damping is more likely to occur at lower global strain/stress amplitudes than amplitude independent dislocation damping. It is to be noted that testing beyond the elastic limit of foams, i.e. micro plastic yielding (Region Ib in Figure 3.9), produces an increase in dislocation density and damping properties are not considered to be stable. One new internal friction mechanism thought to occur in foams is the interfacial friction between defects such as cracks. “Mode conversion”, another new mechanism, is thought to produce amplitude dependant internal friction. Under “mode conversion” the stress Mode may be converted from tensile to shear at the pore boundaries. The shear deformation produces viscous flow with dislocation movement towards pore boundaries and dissipated as heat.

Mechanical Damping characteristics of Aluminum Foam:

The internal friction character of aluminum foam is found to be non-linear, increasing with increasing porosity and decreasing pore size. This is in contrast to the linear internal friction character of bulk aluminum which displays up to 10 times less mechanical damping capacity than aluminum foam when tested at the same amplitudes (1.0 to 2.2 x 10-5). Frequency is found to have no effect on mechanical damping of aluminum foam over a range of 200 Hz to 800 Hz. however a decrease in damping is observed when the frequency was increased from 1 kHz to 3 kHz. Amplitude independent thermo-elastic effects are found to contribute little to the overall damping of aluminum foams. The amplitude dependence and the major source of damping can be interpreted using **Granato-Lücke vibrating string dislocation model** and mode conversion. The difficulties in comparing measured mechanical damping values of aluminum foam tested on different machines are highlighted by the comparison of their results to those produced for the same relative density of aluminum foam.

Mechanical properties of various types of metal foams

Property, (units), symbol	*Cymat*	*Alulight*	*Alporas*	*ERG*	*Inco*
Material	Al–SiC	Al	Al	Al	Ni
Relative density (−), ρ/ρ_s	0.02–0.2	0.1–0.35	0.08–0.1	0.05–0.1	0.03–0.04
Structure (−)	Closed cell	Closed cell	Closed cell	Open cell	Open cell
Density (Mg/m^3), ρ	0.07–0.56	0.3–1.0	0.2–0.25	0.16–0.25	0.26–0.37
Young's modulus (GPa), E	0.02–2.0	1.7–12	0.4–1.0	0.06–0.3	0.4–1.0
Shear modulus (GPa), G	0.001–1.0	0.6–5.2	0.3–0.35	0.02–0.1	0.17–0.37
Bulk modulus (GPa), K	0.02–3.2	1.8–13.0	0.9–1.2	0.06–0.3	0.4–1.0
Flexural modulus (GPa), E_f	0.03–3.3	1.7–12.0	0.9–1.2	0.06–0.3	0.4–1.0
Poisson's ratio (−), ν	0.31–0.34	0.31–0.34	0.31–0.34	0.31–0.34	0.31–0.34
Comp. strength (MPa), σ_c	0.04–7.0	1.9–14.0	1.3–1.7	0.9–3.0	0.6–1.1
Tensile elastic limit (MPa), σ_y	0.04–7.0	2.0–20	1.6–1.8	0.9–2.7	0.6–1.1
Tensile strength (MPa), σ_t	0.05–8.5	2.2–30	1.6–1.9	1.9–3.5	1.0–2.4
MOR (MPa), σ_{MOR}	0.04–7.2	1.9–25	1.8–1.9	0.9–2.9	0.6–1.1
Endurance limit (MPa), σ_e^c	0.02–3.6	0.95–13	0 9–1.0	0.45–1.5	0.3–0.6
Densification strain (−), ε_D	0.6–0.9	0.4–0.8	0.7–0.82	0.8–0.9	0.9–0.94
Tensile ductility (−), ε_f	0.01–0.02	0.002–0.04	0.01–0.06	0.1–0.2	0.03–0.1
Loss coefficient (%), η^c	0.4–1.2	0.3–0.5	0.9–1.0	0.3–0.5	1.0–2.0
Hardness (MPa), H	0.05–10	2.4–35	2.0–2.2	2.0–3.5	0.6–1.0
Fr. tough. (MPa.m$^{1/2}$), K_{IC}^c	0.03–0.5	0.3–1.6	0.1–0.9	0.1–0.28	0.6–1.0

Electrical properties of various metal foams

Property (units), symbol	*Cymat*	*Alulight*	*Alporas*	*ERG*	*Inco*
Material	Al–SiC	Al	Al	Al	Ni
Relative density (–)	0.02–0.2	0.1–0.35	0.08–0.1	0.05–0.1	0.03–0.04
Structure	Closed cell	Closed cell	Closed cell	Open cell	Open cell
Resistivity (10^{-8} ohm.m), *R*	90–3000	20–200	210–250	180–450	300–500

Some experimental studies of energy absorption in a close-celled aluminium foams shows the average values of absorption energy per unit volume of ALPORAS at a strain of 55% for the quasi-static and the dynamic strain rate are calculated to be 1.00 and 1.51 MJ/m^3, respectively. The value of energy absorption at the dynamic strain rate is about 50% higher than that at the quasi-static strain rate. They have suggested that selection of cellular materials for applications such as cycle helmet inner liner, bumper for automobiles or motor cycles can be based on energy absorption.

The compressive behaviour of number of closed cell aluminium foams shows that mean compressive strength increases almost linearly with increasing density. The compressive strength and its scattering are lower for longer specimens due to the higher probability of the existence of a weak link. ZA22 foams was fabricated in 2007 with the melt foaming route using $CaCO_3$ blowing agent and investigated its compressive behaviour. The results showed that SiC particles dispersing in cell walls can alter the deformation mechanism of ZA22 foams. The plateau stress of ZA22/SiCp composite foams fluctuates acutely because SiCp in cell walls alters the deformation mechanism of ZA22 alloy matrix. Closed-cell Zn–22Al foams were also fabricated by melt foaming route using $CaCO_3$ blowing agent. The stress–strain curves of ZA22 foams exhibit three distinct regions: a linear elastic region, a plastic plateaus region, and a densification region. The plastic collapse stress of ZA22 foams increases with increasing relative density. Acoustic emission (AE) response was recorded during compression and indentation of different kinds of aluminium foam and evaluated with respect to the various stages of the deformation process. During compression continuous AE response was measured, while during indentation a

response consisting of individual AE events was monitored. For uniaxial compression they have found that at small strains ($\varepsilon < 0.05$) the foams deform in a linear elastic way by cell wall stretching and cell edge bending. In this regime the deformation was spreading over the entire material. Subsequently, there was a plateau of deformation at almost constant stress (σ_{pl}^{*}), where cells collapse by buckling, yield or fracture of cell walls and cell edges. In the plateau regime deformation is localised in deformation bands: first the largest cells or the cells, which experience the largest stress collapse, then the adjacent cells in a layer which in the case of low relative density foam is perpendicular to the load axis. This will be repeated until all cells in the foam collapse. Finally, there was a stage of densification, where the stress increases steeply as the cell walls crush together. AlSi9Mg composite foams reinforced by SiC particles (SiCp/AlSi9Mg composite foams) was fabricated in 2008 with the direct foaming route of melt using $CaCO_3$ blowing agent. They have studied the static and dynamic compressive behaviour of the composite foams. Their results showed that the yield stress of SiCp/AlSi9Mg composite foams increases with increasing strain rate, the strain hardening occurs during the compression at high strain rate, and SiCp/AlSi9Mg composite foams was more sensitive to the strain rate than aluminium and aluminium alloy foams.

The study of mechanical behaviour of commercially available ALPORAS aluminium foam with two different densities under tension loading shows that the deformation characteristics deviated from those observed in aluminium foams under compression. No deformation bands or plastic instabilities could be observed in tension, which were very frequent in compression of metallic foams. Four regimes were evident in the stress–strain curves and deformation maps: the linear elastic regime, the plastic regime with no significant crack initiation and propagation, the regime of formation of a fracture process zone and, finally, the regime of fracture, where a main crack propagates through the specimen and leads to failure.

Several researches are still carrying out their researches to find the fatigue property of different types of metal foams. Some of the noteworthy works are that of Banhart and Brinkers, (1999), Harte et al. (1999), Zettl (2000), and Golovin et al. (2004). J Ghose (2012) etc.

Fracture behaviour of metallic foams also has been investigated by several researchers. Some important works in this regard are done by Motz and Pippan, (2002), Onck et al. (2005), Amsterdam et al. (2008), and Hong-Wei et al. (2008).

Regarding the assessment of sound absorption characteristics of metallic foams few researches have been carried out. Lu et al. (1999) carried out investigations to determine the sound absorption capacity of Alporas aluminium alloy closed cell foams. To make the foam more transparent to air motion, techniques based on either rolling or drilling were used. They concluded that the as-received cast Alporas foams having closed cells do not absorb sound well and Foams having low initial relative densities are found to be better sound absorbers than those with high relative densities. Jiejun et al. (2003) investigated the damping and sound absorption properties of A356/xSiCp composite foams. They concluded that the sound absorption increases with higher SiC particle volume percent. Kim et al. (2002) investigated the sound absorption properties of aluminium foam developed by them. The found that sound absorption coefficient was low at lower frequencies but high at high frequencies.

Investigations into material processing of metal are yet to be carried out. Miller et al. (2004) investigated machinability of two type of open cell by Wire-EDM process. The two types of metal foams investigated by them were Fe-Cr-Al alloy foam and 316 stainless steel foam. Their experimental results showed that, under the same EDM condition, the 316 stainless steel has higher MRR than the Fe-Cr-Al alloy.

C. Use & Application of Aluminium Metal Foam:

Aluminium metal foam is popular in several sectors. In near future, application of metal foam is going to be increased rapidly. But it is still limited in laboratory & research phase. Some applications are given below--

2.5.1 Orthopedic uses:

Foam metal has also begun to be used as an experimental prosthetic in animals. In this application, a hole is drilled into the bone and the metal foam inserted letting the bone grow into the metal for a permanent connection. For orthopedic uses, foams from metals such as tantalum or titanium are often used, as these metals exhibit high tensile strength, corrosion resistance with excellent biocompatibility.

2.5.1.1 Clinical studies on mammals:

A notable example of clinical use of aluminium foams is a Siberian Husky named Triumph who's both back legs received foam metal prostheses. Studies on mammals have shown that porous metals, such as titanium foam, may allow the formation of vascular systems within the porous area.

2.5.1.2 Orthopedic use in humans:

More recently, orthopedic device manufacturers have started producing devices that use either foam construction or aluminium foam coatings to achieve the desired levels of osseointegration.

2.5.2 Energy absorptional uses:

Aluminium foams are currently being looked at as a new material for automobiles. The main goal of the use of metallic foams in vehicles is to increase sound dampening, reduce the weight of the automobile, and increase energy absorption in case of crashes. Also in military applications, to combat the concussive force of IEDs, in anti-landmine vehicles, bomb disposing vests are made from this material.

The metallic foams that are being looked at currently, are aluminium and its alloys due to their low density (0.4–0.9g/cm^3). In addition these foams have a high stiffness, are fire resistant, do not give off toxic fumes, are fully recyclable, have high energy absorbance, have low thermal conductivity, have low magnetic permeability, and are efficient at sound dampening, especially in comparison to light weight hollow parts. In addition partial addition of metallic foams in hollow parts of the car will decrease weakness points usually associated with car crashes and noisy vibrations. These foams are cheap to cast by using powder metallurgy (as compared to casting of other hollow parts).

In comparison to polymer foams (for uses in automobiles), aluminium foams are stiffer, stronger, and more energy absorbent. They are more fire resistant, and have better weathering properties when considering UV light, humidity, and temperature. However, they are heavier, more expensive, and non-insulating.

Aluminium metal foam technology has also been applied in the treatment of the automotive exhaust gas. Compared to the traditional catalytic converter that uses cordierite ceramic as substrate, the metal foam substrate can offer better heat transfer and exhibits excel lent mass-transport properties (high turbulence) offering possibilities for using less platinum catalyst.

Open cell metal foams are also used in chemical industry as filter where high temperature applications are done. Foams are also used in packaging industries also to package the sensitive and fragile instruments or goods.

Figure 2.25 Isotropic cores for sandwich panels and shells

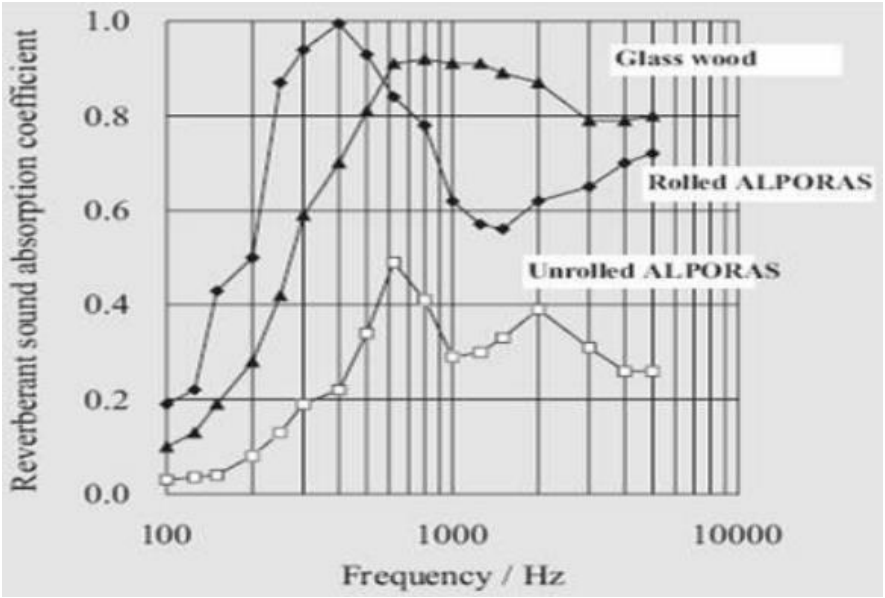

Figure 2.26 Sound absorption of Alporas foam of relative density ~ 0.09

In 1997 use of closed cell aluminium foams for transport industry was introduced. The studies of the compressive behaviour showed that the material exhibits a constant deformation stress and therefore can absorb much more deformation energy than a piece of massive aluminium when both were loaded up to a given limited stress level. The major part of the absorbed energy was

irreversibly converted into plastic deformation energy which was a further advantage of foamed aluminium. At the same stress level the dense matrix material was deformed and it was observed that it releases most of the stored energy after the load has been removed.

A new concept for design and manufacturing of lightweight load-bearing components using metallic foams was introduced in 2007. The concept was based on utilization of complex shaped hollow parts (such as hydroformed profiles or castings) which are (partially) filled with aluminium foam prepared by PM techniques. The utilization of aluminium foam core would increase the capability of component to absorb crash energy in multiple impact directions.

Foamed aluminium panels and sandwiches with aluminium foam core can be potentially used in automotive industry, especially for lightweight stiff body structures of vehicles. The studies revealed that the fracture resistance and damage tolerance can be significantly improved without excessive weight increase by reinforcement with metallic wires, nets or meshes either on one or both panel surfaces (Figure below), which opens an enormous potential for applications in automotive industry especially for lightweight body structures of future cars.

(a) (b)

Figure 2.27: (a) Foamed panel (b) reinforced in the surface with stainless steel mesh

An Austrian car manufacturing company studied the energy absorbing behaviour of aluminium foam absorbing element in A-Pillar system of a real car in 2007. Figure below shows the mounting of the aluminium foam on the test car. They have found that the head injury criterion (HIC) can be reduced by metal foam oriented design.

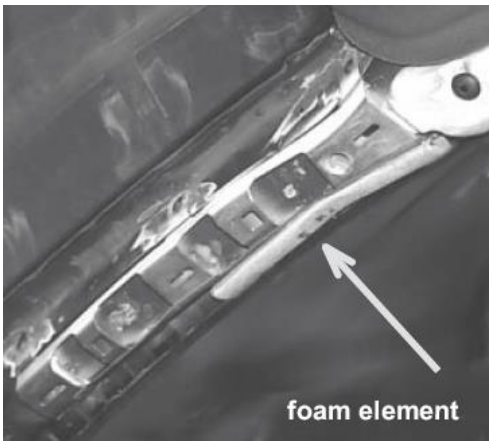

Aluminium foam element mounted on the test car

Motorcycle helmets were designed with metal foam shell and studied their impact behaviour. The biomechanical characteristics of head impact were compared with both metal foam and ABS helmets. The helmet with metal foam shell performs reasonably well compared to ABS helmet.

The use of metallic foam were applied to produce a hip prosthesis in 2011. The Scientists have studied the deforming behaviour of metallic foam and investigated the development of density gradients through a series of experimental forging tests in order to produce a selected portion of a hip prosthesis. Figure below shows the forging process carried by them to produce a hip prosthesis.

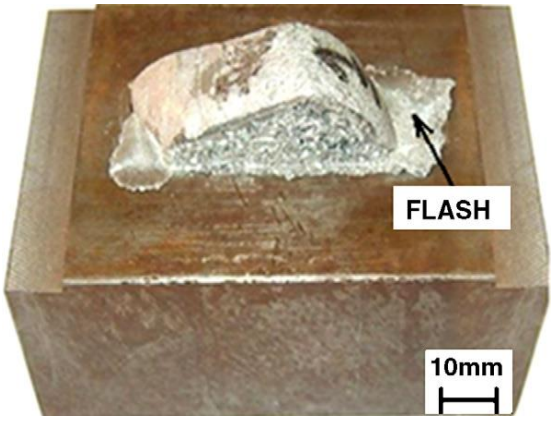

The foam billet at the end of forming process

Banhart and Weaire indicated several application of aluminium foam. They suggested that foam-filled columns or sandwich panels could replace conventional dense metal, e.g. in rotating printing rolls or quickly moving platforms or crossbeams in machines in order to reduce their inertia and to damp vibrations. Biomedical industry could use foams based on titanium as dental

implants since titanium is biocompatible and the elastic properties of the foam can be adapted to the modulus of the bones by selecting appropriate porosities.

Climatizer (Metal Evaporator) was designed in 2012 to preserve the vegetables, fruits etc. It works on the principle that the heat taken away as the heat of evaporation by water through the open cell aluminium foam, which is then taken away by forced convective air flowing through the periphery of the cooling area.

ADVANCED MATERIAL PROCESSING TECHNOLOGY

ME 618

MODEL QUESTIONS:

1. What are metal foams? What are its unique properties?
2. What are the potential applications of Metal Foams?
3. Discuss the advantages and disadvantages of Metal Foams
4. Briefly describe the manufacturing of Metal Foams by P/M technique. What are the advantages and disadvantages of this method?
5. Briefly describe the manufacturing of Metal Foams by investment casting. Give schematic diagrams if necessary. What are the advantages and disadvantages of this method?
6. How metal foams are manufactured by injection of gas in the melt?Give schematic diagrams if necessary. What are the advantages and disadvantages of this method?

7. Write short notes on:
   (i)
   (ii) Various methods of Production of Metal Foams.
   (iii) Cenosphere process of making metal foams.
   (iv) Manufacturing of Metal Foams by compaction of two particles, one leachable.
   (v) Production of Metal Foams by Gas-Metal Eutectic solidification.
   (vi) Compressive behaviour of Metal Foams.
   (vii) Energy absorption by Metal Foams.

ADVANCED MATERIAL PROCESSING TECHNOLOGY

ME 618

ASSIGNMENTS

1. What are the various methods of shaping ceramic materials? Briefly describe their relative advantages and disadvantages. (Kalpakjian, Ch 11, section 11.9)
2. Briefly discuss PVD and CVD process. Give schematic diagrams if necessary. Also discuss their relative merits and demerits. (Kalpakjian, Ch 4, section 4.5)
3. Describe Metal Injection Moulding process with sketch (Kalpakjian, Ch 11)
4. Prove that $P_X = P_0 e^{-4\mu kx/D}$, related Numerical problems (Kalpakjian, Ch 11)
5. Explain the Steps involved in Powder Metallurgy. Describe the phases of sintering.
6. . Briefly describe HIP and CIP process. (Kalpakjian, Ch 11)
7. Write notes on:
   (i) Squeez casting process (Kalpakjian, Ch 5, sec 5.10.5)
   (ii) Rapid Solidification process (Kalpakjian, Ch 5, sec 5.10.8)
   (iii) Atomization process of metal powder manufacturing. (Kalpakjian, Ch 11)
   (iv) Ospray Process (Spray Forming) (Kalpakjian, Ch 11)